Automation & Analysis of Chest X-Ray and Microscopy Image Detection for Tuberculosis

Author

SANA FATIMA

Regn Number

NUST201463156MSMME62414F

Supervisor

DR. SYED IRTIZA ALI SHAH

DEPARTMENT OF BIOMEDICAL SCIENCES & ENGINEERING

SCHOOL OF MECHANICAL & MANUFACTURING ENGINEERING

NATIONAL UNIVERSITY OF SCIENCES AND TECHNOLOGY

ISLAMABAD

DECEMBER, 2017

Automation & Analysis of Chest X-Ray and Microscopy Image Detection for Tuberculosis

Author

SANA FATIMA

Regn Number

NUST201463156MSMME62414F

A thesis submitted in partial fulfillment of the requirements for the degree of

MS Biomedical Sciences

Thesis Supervisor:

DR. SYED IRTIZA ALI SHAH

Thesis Supervisor's Signature: _____

DEPARTMENT OF BIOMEDICAL SCIENCES & ENGINEERING

SCHOOL OF MECHANICAL & MANUFACTURING ENGINEERING

NATIONAL UNIVERSITY OF SCIENCES AND TECHNOLOGY,

ISLAMABAD

DECEMBER, 2017

Declaration

I certify that this research work titled ***"Automation & Analysis of Chest X-Ray and Microscopy Image Detection for Tuberculosis"*** is my own work. The work has not been presented elsewhere for assessment. The material that has been used from other sources it has been properly acknowledged / referred.

Signature of Student
SANA FATIMA
NUST201463156MSMME62414F

Plagiarism Certificate (Turnitin Report)

This thesis has been checked for Plagiarism. Turnitin report endorsed by Supervisor is attached.

Signature of Student

Registration Number

NUST201463156MSMME62414F

Signature of Supervisor

Copyright Statement

Acknowledgements

I am thankful to my Creator Allah Subhana -Watala to have guided me throughout this work at every step and for every new thought which He gave me to improve it. Indeed I could have done nothing without His priceless help and guidance. Whosoever helped me throughout the course of my thesis, whether my parents or any other individual was His will, so indeed none be worthy of praise but He Almighty.

I am profusely grateful to my beloved parents who raised me when I was not capable of walking and continued to support me throughout in every department of my life.

I would also like to express special thanks to my supervisor Dr. Syed Irtiza Ali Shah for his help and support throughout my thesis. I would also like to thank for his cooperation and advice in completing my project.

I would like to thank my co-advisor Dr. Muhammad Nabeel Anwar for her valuable hints and cooperation throughout this research.

I would also like to pay special thanks to Mr. Muhammad Zia surveillance data officer in National TB control program for his tremendous support and cooperation. Each time I got stuck in something, he came up with the solution. Without his help I wouldn't have been able to complete my thesis. I appreciate his patience and guidance throughout the whole thesis.

I would also like to thank Dr.Murtaza Najabat Ali, Dr. Umar Ansari and Dr. Muhammad Naveed for being on my thesis guidance and evaluation committee. I am also grateful for their support and cooperation.

Finally, I would like to express my gratitude to all the individuals who have rendered valuable assistance to my study.

Dedicated to my exceptional parents, to my family and my teacher Mr. Muhammad Zia whose tremendous support and cooperation led me to this wonderful accomplishment

Abstract

TB (Tuberculosis) is a contagious disease which is caused by a bacterium named Mycobacterium Tuberculosis. Mycobacterium Tuberculosis invades the host cell when the immunity of the body gets weakened. TB is an air born infection meaning that the bacterium is transferred through atmospheric air from TB suspect to a healthy person by coughing and sneezing. This bacterium has the tendency to divide rapidly. Screening is done to confirm the presence of TB. There are different screening techniques available i.e. Chest X-ray, Microscopy, Gene Xpert and Culture etc. Medical image processing is a rapidly growing field of image processing that is used to automate different medical procedures. In this research we have designed two automated systems for the screening of TB patients. A sample of 50 sample images of microscopy slides and chest X-ray radiographs were taken. The proposed algorithms were implemented using MATLAB version 9.2. The comparative analysis of results has been done using PASW statistics version 18. The comparison between results from proposed algorithm and reference standard data results was done. The sensitivity of 98% was obtained for chest radiography algorithm and 92% was obtained for bacilli segmentation algorithm. The specificity of 96% was obtained for bacilli segmentation algorithm and 70% for chest radiography algorithm. The accuracy was calculated through Receiver operating curve. The area under the curve was found to be greater for bacilli segmentation algorithm. The proposed bacilli segmentation algorithm gave an accuracy of 94%, whereas the proposed chest radiography algorithm gave an accuracy of 92%. Chi square testing was performed on the two algorithms. The p-value was lesser than 0.05 that showed that the automated techniques are independent form the standard reference techniques. The computation time was lesser for proposed bacilli segmentation algorithm and the method was found to be more reliable for use. The accuracy of the two algorithms was found to be good being above 90, so we can use any of these algorithms for screening of TB patients. These will make the screening process robust and more reliable. Moreover, the proposed systems are expected to reduce laborious fatigue and human errors. The proposed algorithms will assist physicians, doctors and microbiologists in screening of TB patients. Further work could be done to detect other abnormalities of lungs i.e. lung cancer and heart diseases using the proposed chest radiography algorithm. Bacilli segmentation is done on the basis of color, so for future work one could also consider size and shape parameters of bacilli to make the system better.

Keywords: Chest radiography, Smear microscopy, AFB's, True Positives, False Positives, True Negative, False Negatives, ROC.

Table of Contents

LIST OF FIGURES

LIST OF TABLES

CHAPTER 1: INTRODUCTION

In this research the screening procedures for tuberculosis detection are automated for correct diagnosis and treatment of patients.

1.1 BACKGROUND, SCOPE AND MOTIVATION

Tuberculosis is an important health related problem people are facing all around the world. It is an infectious disease that is spread from one person to another though spitting, coughing and sneezing. The samples are of two types either pulmonary or extrapulmonary. Pulmonary samples are taken from inside the lung region and the respiratory tract. The disease is contagious so it can spread to other parts of the body too. The TB in other body parts is called extrapulmonary Tuberculosis. Our research is mainly based on lung region. The presence of mycobacterium tuberculosis in smear slides gives an indication of the presence of tuberculosis disease in the patient. We will focus on pulmonary tuberculosis effecting major parts of the lungs.

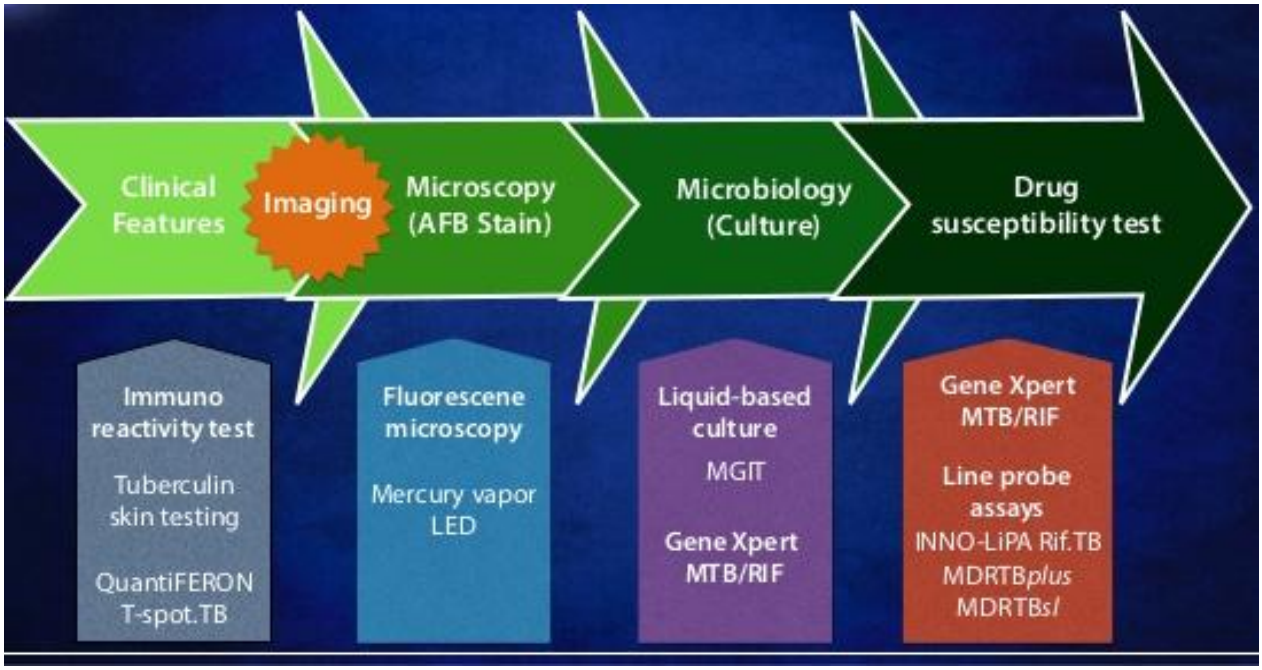

Figure 1: This figure shows a flow diagram for confirmatory procedures and diagnosis of TB. Microscopy and Imaging (CXR's) are automated in this research study. Microscopy is shown in green and imaging in red. These tests are performed in laboratory after clinical features testing. [28]

Tuberculosis is cured if diagnosed properly through tests and medicines. For the diagnosis and screening of tuberculosis different methods are available as shown in figure 1. These tests includes chest radiography, microscopy, genexpert, culture, drug susceptibility test and line probe assay test. The initial screening starts from the chest radiography and microscopy test. The advance testing will then include Genexpert, culture, drug susceptibility and line probe assay test.

Mycobacterium tuberculosis is the bacterium causing tuberculosis. The surface region of mycobacterium tuberculosis is covered with waxy coating. The coating of the surface is waxy due to the presence of Mycolic acid and is not affected by gram staining. Acid fast stains e.g. fluorescent and Ziehl-Neelsen (ZN) stains are used for identifying mycobacterium tuberculosis. The shape of mycobacterium tuberculosis is slightly curved and straight appearance. The length of mycobacterium tuberculosis is 1-10 μm and width of 0.2 to 0.6 μm. [1]

Image processing is a rapidly growing field of study. Image processing toolbox of Matlab consists of different functions that are used for interpreting and analyzing the data of different images. The data is used for obtaining region of interest and exploring important information from the images. Medical image processing is an important branch of image processing used for biomedical research. Medical image processing enables medical professionals in diagnosing and treating against different diseases. The data in the images can be used to obtain quantitative and qualitative information of the patients suffering from different types of diseases. Different equipment's have been designed e.g. MRI, CT scan, PET and digital microscopy are designed for performing medical examinations for different diseases.

The screening of tuberculosis through chest radiographs is inexpensive. The analysis and interpretation of CXRs is prone to errors and depend on the expertise of the specialist. Moreover, screening of tuberculosis performed manually is laborious and time consuming. Medical image processing tools can be used to automate the screening process of tuberculosis. The automated

system will help in improving the screening process of tuberculosis in less time and reduces the chances of errors.

The microscopy and chest radiograph images are used as an input for the two different proposed algorithms. In our study we are performing confirmation for pulmonary tuberculosis through the designed algorithm. The statistical analysis is performed to find the accuracy and reliability of the algorithm. The specificity and sensitivity of the designed algorithms will also be analyzed. The ROC interpretations will be done and chi square test will be performed.

1.2 RESEARCH OBJECTIVES:

The main objectives of this research are:

- To propose a computational approach for screening tuberculosis patients.
- To design a system that can detect mild and severe form of tuberculosis.
- To identify Acid fast bacilli in microscopy slide images computationally.
- To perform statistical analysis for detecting the efficiency and robustness of the system.

CHAPTER 2: LITERATURE REVIEW

Different approaches of image processing have been used in the past for automation of chest radiography and microscopy. The research on automated screening of tuberculosis has provided various methods for predicting the disease.

2.1. RESEARCH FINDINGS OF AUTOMATED CHEST RADIOGRAPHY

The screening of tuberculosis of large population is a time consuming and difficult task. A fully automated system for chest radiograph detection was designed using local textural analysis approach. The study was done on frontal chest radiographs and an abnormality score was obtained. The algorithm detects diffuse textural features in mass chest X-ray screening process. In the first step active shape model is used to perform segmentation. In the step of segmentation the region of interest is subdivided into overlapping regions of different sizes. The texture features are extracted to a multiscale filter bank. The feature vectors are subtracted from corresponding regions in the right and left lung fields to obtain difference features. For each region a separate training set is made and classification of all regions is done among the nearest neighbors. A weighted multiplier is used to combine classification results for each region. The higher classification regions weigh more and are used to produce an abnormality score for each image. The system was evaluated on two databases. In the first database 241 normal images and 147 images with textural abnormalities were taken for evaluation of algorithm. The sensitivity of 0.86 and a specificity of 0.50 were obtained. The area of receiver operating characteristic curve of 0.820 was obtained. The second database consists of 100 normal images and 100 abnormal images. The sensitivity of 0.97 and specificity of 0.90 was obtained with the area under the receiver operating curve of 0.986 from the second database. [2]

The Cavities present in the lungs shows the disease of highly infectious nature. In upper lobe of the

lung region the presence of cavities gives an indication for the presence of an infection. The process of cavity identification is halted by the presence of superimposed structure in the lung fields of anatomical nature. The system was designed for cavity detection that uses coarse to fine dual scale method. The gradient orientation features, local binary pattern and Gaussian based matching attributes are utilized at the coarse scale level. However at the fine scale level gradient inverse co-efficient of variation, kullback-leibler divergence and circularity are utilized for designing this computer aided system. The system designed will be dual scaled coarse to fine classification method for tuberculosis cavity detection. The designed method surpasses the existing methods because the textural, gradient and textural features are considered in the designing of algorithm. Secondly, the accuracy of the system is improved by incorporating fine scale contour feature classification. The contour features include edge, region and shape. Thirdly, the segmentation process is improved by enhancing the contours by incorporating Hessian matrix based image enhancement. The system designed is used in the diagnosis of the disease because of the higher detection rate. The sensitivity of 78.8%, specificity of 86.8% and accuracy of 82.8% is achieved by adding contour features and by using more specific knowledge. [3]

The overlapping structures present in different regions of the lungs makes automated detection process difficult. The Chest radiographs with textural abnormalities were detected by two Computer aided detection systems designed. From the two systems designed, a system was tested on normal CXR's images and another system was tested on bone suppression images. The software named ClearRead 2.4 was used for creating bone suppression images. The test was conducted on 431 normal and 434 abnormal images. The abnormal regions were assigned rates and then evaluated. An independent dataset containing 900 images were taken to evaluate the performance of the system for normal and abnormal regions of the lungs. The dataset contains 1127 abnormal and 454 normal regions. The abnormal regions are divided into three categories containing 320, 527 and

280 abnormal regions. The average abnormality score for normal regions of p=5.6*10-19 was obtained. The average abnormality score for abnormal regions of p=0.73 for category1, p=5.7*10-19 for category 2 and p=4.4*10-7 was obtained. In the case of normal regions the CAD score slightly decrease in case of bone suppression images. However, for abnormal regions the score slightly increases. The use of bone suppression images results in improving the detection system for textural abnormalities which was a challenging task.[4]

Another important research was conducted to investigate the textural properties of tuberculosis related anterior-posterior and normal chest radiographs. A snake guided algorithm was proposed for the segmentation of the field of interest. The information of pixel data corresponding to the field of interest was extracted. The characteristics of normal and tuberculosis images were analyzed by the gray scale intensity distribution present in the region of interest. The characteristics studied are then imparted to the classifiers for automated classification. The statistical analysis of chest radiographs intensity distributions had shown higher entropy, variance, third moment and a lower mean value for tuberculosis images as compared to normal ones. A decision tree based adaboost classifier adjunct tool was trained and the accuracy of 94.9% was obtained for classification of tuberculosis chest radiographs. The normal and tuberculosis based chest radiographs were discriminated by an integrated index known as tuberculosis index on the basis of texture features. This tuberculosis index will be used as a tool for the routine screening of tuberculosis patients by the radiographers. [5]

Screening of chest radiographs can also be done using another approach of combined lung masks. In this research the data was taken from two different data sets. One set was combined by Japanese society of radiological technology (JSRT) and another set was obtained from local department of Montgomery County (MC), Maryland. The JSRT data comprises 247 chest x-rays of

which 93 x-rays were normal and 154 x-rays are abnormal. The MC set contains 138 x-rays from which 58 x-rays were abnormal and 80 were normal. The difference between the two datasets was that the JSRT Dataset contains only nodules however the MC Dataset comprises a wide range of abnormalities. The data is inputted to the algorithm to extract the lung field for performing classification. Lung segmentation was performed by using three different types of lung masks. The intensity mask, the lung model mask and Log Gabor mask were used for lung segmentation. The average of the three masks gave us an overall lung segmentation mask. The threshold was set at 0.5 and the pixels of value greater than 0.5 is considered as part of the lung. The detect normal and abnormal patterns in the segmented lung fields, a set of texture and shape descriptors were used which can identify features. The features were used to train a linear support vector machine system for screening of chest radiographs. The system provides an area under the curve (AUC) of 83.12% by combine use of the three segmentation masks. The accuracy of 75% was achieved using this algorithm.[6]

The severity of tuberculosis disease can be studied in chest radiographs. The process of segmentation is done using particle swarm optimization approach. The segmented image is used as an input to the feature computation process. The feature computation process mainly performs computation for the intensity features of the segmented image. The mean of all the intensity levels is taken for calculating the contrast of the segmented image. The standard deviation is taken for measuring the brightness of the image. The proposed system uses support vector machine classifiers for patterns recognition and data analysis. The chest radiograph is detected as normal or abnormal by support vector machine classification system. The input of support vector machine classifier is received by the severity analysis process. The intensity value and the classification of the disease will be used to detect the severity of the disease present in chest radiographs. This is the major

advantage of the designed methodology that it will provide the medical professional with the knowledge of severity of the disease.[7]

Another important system was designed for automated screening of tuberculosis using MATLAB image processing tools. The chest radiographs were taken as input for performing segmentation. The active contour approach was used for segmentation of lung regions. A set of statistical features e.g. mean, standard deviation, skewness, entropy and kurtosis were used as an input to the classifier. The classifier on the basis of these statistical features classifies the image as either normal or abnormal. The values of variance, entropy and third moment features were lower in case of normal chest radiographs however the value of mean was greater. In case of tuberculosis chest radiographs the value of mean was greater however the values for other statistical features were higher. The infection is spread asymmetrically in case of tuberculosis. Therefore, there is a greater disparity on every feature value between the right and left lung of tuberculosis chest radiograph. [8]

The cavities present in the upper lung regions is an indicator of tuberculosis infection. A system was designed for the automated tuberculosis cavity detection. The proposed system consists of four modules that are Hessian matrix based image enhancement (HIE), Gaussian model based template matching (GTM), segmentation, classification and feature extraction. The GTM was used for finding the cavities without performing any modifications with the image. The HTM module then improves the image quality. The Hessian matrix based image enhancement is combined with 2D Gaussian model based template matching for performing segmentation and features extraction. However the geometric features e.g. circularity is needed to be extracted. The circularity thresholding is done for classifying the images as either normal or abnormal. The results had shown that in proposed system the true positive rate was incremented upto 13%. The missing rate and false

positive rate was decreased to 13% and 4% as compared to other hybrid methods. Moreover, the segmentation results were improved to 8% with the help of Hessian based image enhancement module. [9]

A research was done in which an automated chest radiography system was compared with manual interpretation by the clinical officers. The system was designed named CAD4TB for the automated detection of tuberculosis. For using CAD4TB, 161 images were given abnormality scores in the range 0 to 100. The clinical officers interpreted the images and abnormality scores were assigned consistent with the tuberculosis disease. The Result of CAD4TB and clinical officer's interpretation results were compared. The area under the receiver operating characteristics curve was 0.91 for CAD4TB and 0.89-0.94 for clinical interpretation. There was no significant difference in P values of the results. The kappa statistics value was 0.61 for CAD4TB. The Kappa statistics value for clinical results lies in the range between 0.49-0.67. Therefore, CAD4TB can be used for testing and examination of tuberculosis patients. [10]

Different CAD systems are designed for dealing with imaging modalities for the diagnosis and treatment of different diseases. The presences of cavities in the lungs often suggest the presence of tuberculosis. The geometrical, demographic and spatial information is useful in identifying classification and segmentation of TB cavities. A hybrid Bayesian classification approach is used for automatically detecting TB cavities in identifying infected lungs. The circularity measures and inverse of gradient variation coefficient are used for detecting and classifying TB cavities. The accuracy of 82.35% was obtained. The result of the segmentation technique was compared with other classical active contour technique and nonhybrid approaches. The TB cavities were difficult in identification through other techniques due to the presence of complex tissue pattern however bayesian classification approach detected cavities with false positive rate of 0.05 per image. [11]

A research was conducted for developing countries and communities where resources were limited. A registration driven non rigid lung segmentation approach was used in designing an automated system for diagnosis of tuberculosis using digital CXRs. A patient specific lung models were used for the detection of boundaries of the lungs. The system performs the tasks in three main steps. An image retrieval approach was used that was based on the contents of the image. The training images that were masks based were used to match with the patients CXRs using Bhattacharya similarity measure and radon transform measure. A radon transform is used for reconstruction of images using integral transform. An integral transform is used to output another function from the input function. Bhattacharyya measure was used to measure similarity between the original CXR image and masked image. The second step was to create lung shape model using SIFT flow. The SIFT flow algorithm is used for matching features of two images. The third step was the extraction of lung boundaries using customized energy function. An average accuracy of 95.4% was obtained. The algorithm was also tested on two other datasets on which the accuracy of 94.1% and 91.7% was obtained showing the robustness of this lung segmentation approach. [12]

2.2. RESEARCH FINDINGS OF AUTOMATED SMEAR MICROSCOPY

Smear microscopy is a method for detecting the presence of TB bacteria in the samples of patients. This is a manual system for testing the presence of tuberculosis. Different automated techniques had been designed with the invention of digital microscope.

Image processing approaches of k-means clustering and Otsu thresholding were used for segmenting TB bacilli. A research was done to check the comparison the two approaches. Thresholding is used to reduce the number of gray levels or colors from the image. A threshold value is assigned to the pixels of the image. The values of intensity larger than the assigned threshold are the object point. All the remaining points are called background points. The second

approach used in this paper is K-means clustering algorithm. Clustering is done to assign the observations into subsets and the subsets are assigned clusters by similarity between them. The comparison of the two approaches showed that the results of K-mean clustering approach were better. The accuracy of 98.91% was obtained using K-mean clustering approach. However Otsu thresholding showed an accuracy of 98.36%. The specificity of 99.22 and specificity of 98.73 was obtained using clustering approach. [13]

A study was conducted for screening of tuberculosis using color spacing. The images were processed on the basis of color and size information to obtain the object of interest. Bacteria are the objects of interest. Color spacing was used to transform the images into YIQ color space. Y color is for luminance, I for hue and Q for saturation. Y color space is for grayscale information and the other two are for color information. For further examination canny edge detection was applied to Q layer along with mathematical morphology. Canny edge detection method is used for identifying edges in the image and mathematical morphology is used for describing shapes in the image. A pattern recognition classifier was used to obtain final bacilli discrimination. The results showed 90% specificity. [14]

An improved diagnostic system was designed for identifying bacilli automatically. A digital microscope was used for capturing the images. It was combined with another autofocussing and bacilli identifying algorithm. The images are captured and processed in real time for identifying bacilli. The numbers of bacilli are also counted by this system. The image capturing algorithm judged whether the microscope is properly focused. This is done by a comparison of focus measures in two adjacent images. In focus measurement the overlapped regions are taken into consideration. HSV color spacing was used for segmentation. HSV color spacing can distinguish color families correctly. A CIE L*a*b* color space is also used for segmentation to increase the accuracy as it

closely resembles to human lightness perception. The shape of the objects can be preserved using CIE L*a*b* spacing. A two stage segmentation system was designed. The tuberculosis bacillus is identified using three descriptors. The three descriptors are compactness, area and roughness. The true bacilli are counted on the basis of decision tree. The sensitivity of 100% and specificity of 94% was obtained. [15]

A color thresholding based algorithm was designed for segmentation of ZN slide images. The color of the bacilli is the most important factor to be considered for this study. The threshold value was assigned on the basis of bacilli color. A slight modifications and adaptions were done and a multilevel thresholding was conducted. Segmentation was done to remove most of the unwanted pixels from the image. The image pixels similar to tuberculosis bacilli were retained. The results of the algorithm showed that the segmentation method was able to filter out the bacilli using the suitable threshold value. [16]

An approach was designed for ZN based stained tissue Images. Image processing was used with neural network in this algorithm. A light microscope was used to capture images. K-means clustering is used to separate bacilli from the image. The quality and speed of the segmentation procedure was improved by using C-Y and RGB color spacing. Feature extraction process is done by measuring Zernike moments and by using hybrid multilayered perceptron network. Zernike moment is a feature descriptor that is used to extract features from the image. A multilayered hybrid perceptron network is used in neural networks and is used in this algorithm to improve the accuracy. The accuracy of 98.07% was achieved using this algorithm. [17]

An algorithm was designed for pulmonary diagnosis of tuberculosis. The algorithm segments, detects and quantify the number of bacilli in sputum smear digital images. The sputum smear samples were prepared using ZN technique. In the segmentation step different color spaces

were taken in consideration for making the algorithm efficient and accurate. The RGB, YIQ, HSV, LAB and YCbCr color spacing techniques were used to reduce illumination variations and noise. The quantification of bacilli was done by determining average bacilli size. The observations show that Lab and YCbCr color spacing performs better with a specificity of 100% and sensitivity of 90.9% was obtained. The accuracy of the system was 85.7%. This shows that according to the given infection level the algorithm provides correct diagnosis of greater than 85%. [18]

Bacterial segmentation is an important step for the screening of the disease. A method was developed for segmentation and classification of TB bacilli. The ZN stained slide images were used as an input. The hue component of the image was assigned a threshold on the basis of appropriate range. The saturation component identifies beaded bacteria. The thread width, area and length parameters chosen for threshold and beads can accurately identify true bacilli. [19]

Adaptive thresholding is another way of segmenting objects. It takes a color or grayscale image as an input and a binary image is the output. A method involving global adaptive thresholding was used in an algorithm for segmentation. RGB color format is a key to this method and subtraction of green from red images was done. After segmentation some of the artifacts are present in the images that are removed using size, morphological and size filters. A sensitivity of 76.65% was obtained. [20]

Screening process can also be automated by using classifiers. A classifier based algorithm was constructed using pixels of the image. A two class pixel classifiers were used for segmentation. For extracting bacilli features Fisher transformation and subset selection methods were employed. The two classifiers are compared. The sensitivity and specificity of above 95% was obtained for all tested classifiers. [21]

A color based Bayesian segmentation is another method for identifying possible TB objects. The probabilities of pixels were derived from a probability density function histogram. Most of the bacilli pixels were red, blue and green color. The pixels color of bacilli was different from non TB objects. Thresholding of pixels created a binary mask. This mask was improved using the structuring element. The features were extracted on the basis of shape of the bacilli. Two types of shape descriptors that include axis ratio and eccentricity were used. The designed approach has several benefits that include the targeted ZN method used globally. The method works in the presence of several artifacts. The shape selection procedure that is size invariant makes the system robust. The software can work on personal computers because of the simplicity of the algorithm and it can be easily modified. [22]

Luminance, saturation and hue are color ranges with different illumination. They are used to generate different color models. A color model based algorithm was designed for screening and confirmation of bacilli. The NTSC saturation color model is extracted to perform color segmentation. Otsu method is used for thresholding the image pixels. The feature and shape of bacteria are extracted by two parameters i.e. compactness and eccentricity. The recognition of object and training of dataset is performed using support vector machine approach. The results of algorithm counting matched with the manual counting results. [23]

Image processing is used with neural network for the identification of bacilli. Segmentation is a process of dividing an image into parts. In this study the algorithm is based on two characteristics. The characteristics are discontinuity and similarity. De-correlation stretching is done to separate colors in a multichannel image. The stretching function is used for visual analysis and making feature judgment easier. The shape and structure of the tuberculosis objects are extracted using morphology. Morphology comprises of two main steps that are erosion and dilation. The descriptor

e.g. eccentricity and compactness are used and 929 types of bacilli shapes are taken as an input to neural networks and identify TB bacteria. The accuracy of 88% percentage was obtained. [24]

This research is a continuation of a survey for different automated techniques already designed. The table 1 given below contains information of different designed approaches with their significance and limitations. [29]

Table 1: Summary of Automated detection Methods for screening of tuberculosis patients. [29]

Authors	Approach	Dataset	Method	Accuracy	Limitation
Cicero Ferreira Fernandes Costa Filho, Luciana Botinelly Mendonça Fujimoto, Pamela Campos Levy, Clahildek de Matos Xavier, Marly Guimaraes Fernandes Costa.[31]	Scalar Selection technique and filtering.	120 sputum smear images of 12 patients.	Automated Smear Microscopy detection.	96.80% Sensitivity.	Error rate of 3.38%.
Hrudya Das and Ajay Nath.[32]	Region based active contour segmentation and support vector machine.	138 Posterioanterior Chest X-rays.	Automated Chest X-rays detection.	No accuracy value given just showing detection approach.	When increasing the features selected and when using another segmentation method it may get more accurate result.
Ajay Divekar, Corina Pangilinan, Sean Kennedy, Tarlochan Sondh, Fleming Y. M. Lure and Gerrit Coetzee. [33]	Stepwise Classification approach.	176 Sputum smear microscopy slides.	Automated Smear Microscopy detection.	Accuracy of Negative detection was 88.24%, accuracy of Scanty detection was 56.00%, and accuracy of High-concentration was 97.96%.	Not mentioned.
Jhanshy. J, Prof. S. Pushparani. [7]	Particle Swarm Optimization.	Not Available.	Automated Chest X-ray detection.	No Accuracy is mentioned.	Not mentioned.
P. A. Kamble, V. V. Anagire and S. N. Chamtagoudar.[13]	Lung decease classification.	Not available.	Automated chest X-ray detection.	No accuracy is mentioned.	Not mentioned.
Julius Santony and Jufriadif Na'am [45]	Math Morphology and Feature Region Analysis.	A total of 40 X-ray images are usd.	Automated chest X-ray detection.	Not mentioned.	Not mentioned.

Authors	Approach	Dataset	Method	Accuracy	Limitation
Jeannette ChangPablo ArbeláezNeil SwitzClay ReberAsa TapleyJ. Lucian DavisAdithya CattamanchiDaniel FletcherJitendra Malik. [34]	Support vector machine classification.	594 images corresponding to 290 patients.	Automated Smear microscopy detection.	Average precision of 89.2% ±2.1% was obtained.	Not Mentioned.
P. Sadaphal, M.F. Beg, G. W. Comstock, and J. Rao. [35]	Color based Bayesian Segmentation.	Not mentioned.	Automated smear microscopy detection.	No Accuracy is mentioned.	Clusters superimposition, low field depth and variations in stain were challenges.
Chandrika V, Parvathi C.S., and P. Bhaskar. [22]	Smoothening sharpening and edge detection algorithm.	A total of 80 chest X-ray images.	Automated chest X-ray detection.	Accuracy rate of 91.25%, sensitivity rate of 90.48% and specificity rate of 92.11% was obtained. Accuracy was improved to 16.18% using this method.	The Target error of 0.003 was obtained.
Amarja Adgaonkar , Juhi R. Nath, Aditi Atreya and Akshay D. Mulgund, . [36]	Sobel algorithm and neural network classifier.	Not available.	Automated smear microscopy detection.	93.5% sensitivity.	The work done can be extended in the Hybrid development algorithm.
Joshua M. Leibstein and Andre L. Nel. [37]	Local binary pattern classifier.	Not available.	Automated chest X-ray detection.	Not mentioned.	Not mentioned.
Prabhat Gupta, Malay Kishore DAyush Goyal, Mukesh Roy, utta, Sarman Singh and Vandana Garg. [38]	Tubeness filtering and Otsu Thresholding.	Not available.	Automated smear microscopy detection.	Not mentioned.	Not mentioned.
Manuel Forero-Vargasa,Filip Sroubekd,Josue Alvarez-Borrego,Norberto Malpica,Gabriel Cristobal,Andres Santos,Luis Alcala, Manuel Desco, and Leon Cohen. [39]	Color filtering and fuzzy segmentation.	25 Sputum smear images.	Automated smear microscopy detection.	82% specificity.	Not mentioned.
Ibnu Siena , Kusworo Adi , Rahmat Gernowo and Nelly Mirnasari. [40]	De-correlation stretching and hidden layer neural networks	929 TB bacteria shape.	Automated smear microscopy detection.	88% Accuracy.	Improvements required in pattern recognition.

Authors	Approach	Dataset	Method	Accuracy	Limitation
Rethabile Khutlang, Sriram Krishnan, Ronald Dendere, Andrew Whitelaw, Konstantinos Veropoulos, Genevieve Learmonth and Tania S. Douglas. [21]	Kohlar illumination and pixel classifiers.	19 Smear Positive slides were taken and a total of 100 images were obtained from 19 different patients.	Automated smear microscopy detection.	The sensitivity and specificity of above 95% was achieved.	There is a need for Searching descriptive and touching bacillus.
Kim Le. [30]	Watershed Segmentation.	100 CXR's.	Automated Chest X-ray detection.	Not mentioned.	Tuning of the system designed is further in process and can be extended to other chest diseases.
Kusworo Adi,Rahmad Gernowo, Aris Sugiharto, K. Sofjan F, Adi P, Ari B. [23]	Otsu Thresholding and support vector machine algorithm.	929 images are taken.	Automated smear microscopy detection.	Not mentioned	Not mentioned.
Rachna H. B. and M. S. Mallikarjuna Swamy [46]	K-means clustering and Otsu Thresholding approach.	25 positive tissue slides.	Automated smear microscopy detection.	K-means clustering approach gave 98.91% accuracy and Otsu Thresholding approach gave 98.36% accuracy. However clustering is the best method as it is highly sensitive to the TB pixels.	Not mentioned.
R.K.Manisha, K.S.Palanisamy [48]	Graph cut lung segmentation.	Not mentioned.	Automated Chest X-ray detection.	Not mentioned.	Different features are extracted from chest radiograph and classifiers will be used to improve performance of the system.
Rethabile Khutlang, Sriram Krishnan, Andrew Whitelaw, and Tania S Douglas [47]	One class pixel and object classifier	Nineteen ZN-stained sputum smear slides.	Automated smear microscopy detection.	The sensitivity of 97.89% and specificity of 94.67% was obtained.	Not mentioned.
Pragnya Maduskar, Rick H.M.M. Philipsen, Jaime Melendez, Ernst Scholten, Duncan Chanda, Helen Ayles, Clara I. Sánchez and Bram van Ginneken [44].	Random forest based detection classifiers.	A total of 638 CXRs are used.	Automated chest X-ray detection.	Not mentioned.	Not mentioned.

Authors	Approach	Dataset	Method	Accuracy	Limitation
Stefan Jaeger, Alexandros Karargyris, Yi-Xiang Wang, Sema Candemir, Les Folio, Jenifer Siegelman, Fiona Callaghan, Rahul K. Singh, Zhiyun Xue, Kannappan Palaniappan, Sameer Antani, George Thoma, Pu-Xuan Lu, and Clement J. McDonald [41].	Binary classifier system.	Dataset consisting of 138 CXR's.	Automated chest X-ray detection.	82% accuracy was achieved.	Performed on limited dataset.
Hogeweg L, Sánchez CI, Maduskar P, Philipsen R, Story A, Dawson R, Theron G, Dheda K, Peters-Bax L, van Ginneken B [24].	CAD system with several subscores of supervised subsystems.	Two databases each consisting of 200 digital CXRs.	Automated chest X-ray detection.	Not mentioned	Differences in the performance of the combined TB Score and independent observer were not significant in both databases.
Wan Siti Halimatul Munirah Wan Ahmad, Mohammad Faizal Ahmad Fauzi and W Mimi Diyana W Zaki [43].	Abnormality scores are detected based on symmetrical lung area, sharpness of costophrenic angle, area of the lung and the lung level.	212 normal and with diseased radiographs.	Automated Chest X-ray detection.	78% of the infection and 100% of the fluid images are correctly detected as abnormal.	Not mentioned.
D.Jeevitha, J.Rajasekaran [47]	Histogram based Parallel Pixel Segmentation.	Two different feature sets.	Automated chest X-ray detection.	Not mentioned	Not mentioned.

CHAPTER 3: METHODOLOGY

This research work has two important parts. The automation of screening procedures for tuberculosis has been performed. In the first part a Chest x-ray algorithm has been proposed for screening of abnormality in tuberculosis patients. In the second part, Acid fast bacilli detection in microscopy slide images has been done. Statistical analysis was performed for the algorithms to check the accuracy and usefulness.

3.1. DATA COLLECTION

A total of 50 patient's samples were obtained for chest radiography and sputum smear microscopy. The data was collected from Federal Government services Hospital Islamabad, Pakistan. The original data of smear microscopy and chest radiography was used as reference standard. Sputum smear microscopy and chest radiograph images were selected for the algorithm designing. The sputum smear slides used for this study were ZN stained. ZN staining was preferred as it is cheaper and easily available as compared to Fluorescence staining that is more expensive.

3.2. IMAGE ACQUISITION

The machine performing radiography was having the capability to convert images into computer readable form in two dimensional formats. The depth information is lost however the height and width is restored. The size of chest radiographs was 3000*2400 with the width of 3000 pixels and length of 2400 pixels. The resolution of chest radiographs was 72 dpi.

The sputum smear microscopy images were gathered using a digital microscope named LABOMED Lx 400 (ivu3100) of NUST University from Biochemistry lab of the department of Bio-medical Sciences & Engineering. The images were gathered using pixel pro software. The microscope used was set at a magnification of 100X. The size and resolution of the image for

microscopy images was 800*600 pixels with a width of 800 and length of 600 pixels. The horizontal and vertical resolution was 300dpi.

3.3. IMAGE PROCESSING

The Images were processed using MATLAB R2017A with version 9.2. It provides a computing environment for the implementation of different algorithms. It is a software used for a wide set of applications. The algorithms were implemented using image processing techniques in MATLAB. The schematic diagram is the methodology is shown in figure 2.

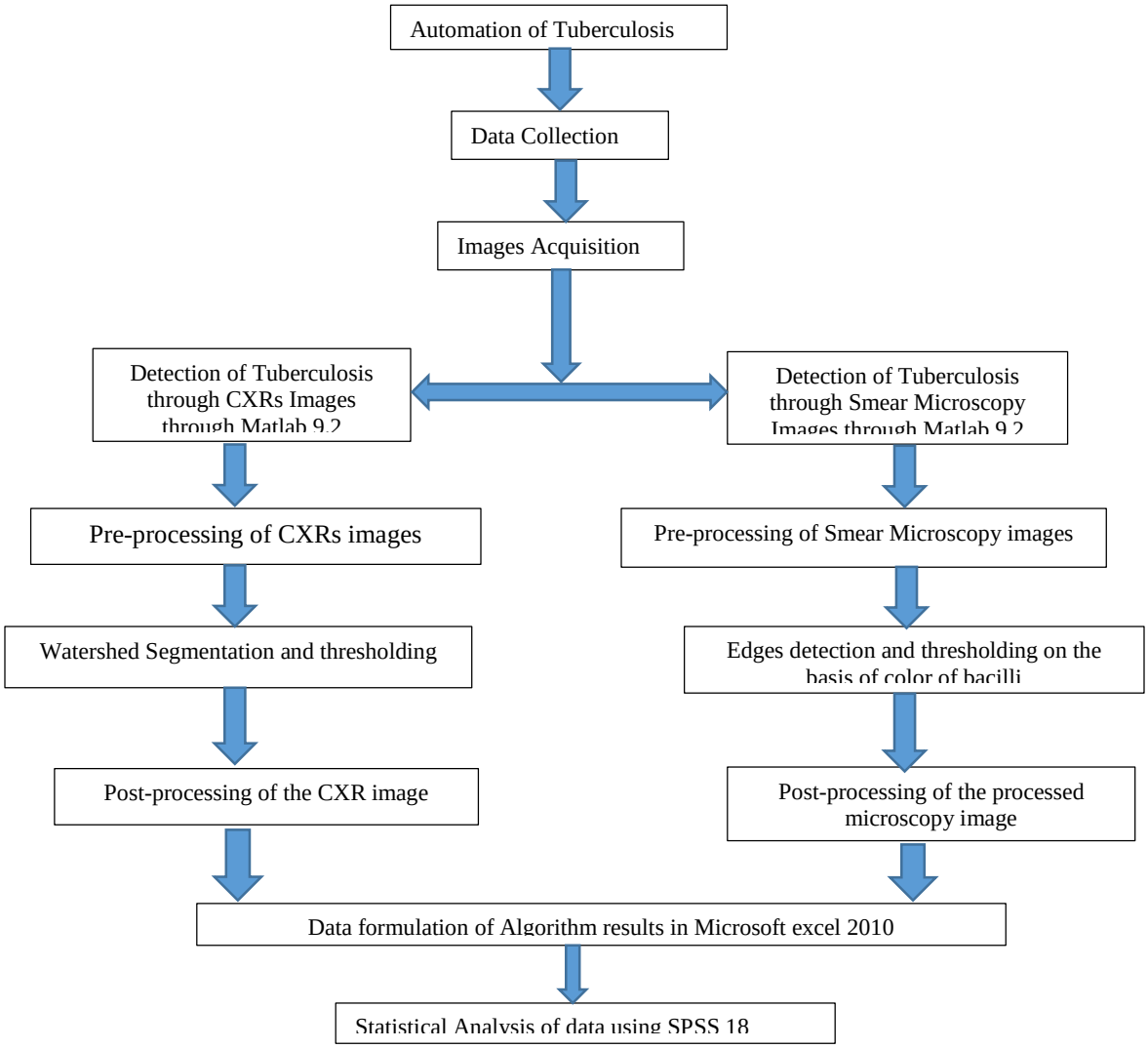

Figure 2: This figure shows schematic representation of methodology for automated tuberculosis detection and analysis.

3.4. AUTOMATION OF CHEST RADIOGRAPHY

Automation of chest radiography was done using watershed segmentation approach. The CXRs of patients were examined by a pulmonologist of Federal government services hospital, Islamabad and this information was taken as reference standard for detecting the disease. The following steps were implemented for the identification of abnormality.

➢ PREPROCESSING FOR LUNG ISOLATION

Preprocessing of the images is done to focus the region of interest.

- A dataset containing 50 CXR images were used for preprocessing using MATLAB software. After reading, the format of the images was deduced from its content.
- A for loop was applied for robustness on 50 images to identify abnormality in all the images iteratively.
- The contrast of images was improved using imadjust function. The new intensity values are assigned according to the low and high intensities of the original image.
- The original size of the images was 3000*2400 Pixels. For fast processing, the image is scaled down to 500*500 pixels using imresize function.
- The image is further cropped to 400*400 to remove head and arm area and focusing the lung region as the study is on pulmonary samples.
- All these steps are considered for preprocessing the CXR images.

➢ WATERSHED SEGMENTATION AND THRESHOLDING

Watershed segmentation was used to separate the two lungs from the background. The lung objects are then detected and abnormality is identified.

- The process of segmentation starts from the minima and proceeds towards maxima values. The core regions of the lungs are the minima and the boundaries are maxima. This is water-flow process i.e. water flowing from valleys and mountains.
- Histograms for the CXR images were generated using histogram function to identify the ranges of the grayscale. A total of 6 gray levels are selected on the basis of histogram.
- Gray levels are used to sort the pixels in to five regions. Each region had a specific percentage of the pixels. A numerical score is assigned to different regions on the basis of pixel percentages. This numerical score is categorized into dark and bright thresholds. Dark thresholds are the core region of the lungs.
- The bright thresholds are the dark background and bright background parts covering the boundaries of the lungs.
- The core regions of the lungs which are assigned darker threshold are used as starting point and the algorithm proceeds iteratively.
- The designed algorithm slowly increments the dark threshold and decrement the bright threshold.
- The algorithm proceeds iteratively until no more pixels are left to be marked.
- The pixels of the CXR image were classified into three components i.e. bright background, dark background and lung objects.
- Similarly a drying process is implemented which is the reverse of water flowing pattern. In this part algorithm starts from maxima and flow towards minima. This step pushes the lung boundary towards the core region of the lungs.
- In this way whole of the lung is isolated for examination.

- The Screening of the lungs is done through a small window of fixed size called a scanning window.
- The window is applied to every pixel of lung object having gray level greater than the threshold.
- The maximum and the average gray levels were calculated. The threshold value is taken between the average and maximum gray levels.
- The gray level values higher than the threshold are marked and counted.
- If the value is between the ranges of high and low thresholds it means there is a possibility of the presence of abnormality.

➢ POST PROCESSING

- The greater number of pixels marked by the algorithm will be categorized as the major form of Tuberculosis. Similarly, lesser number of marked pixels will be considered as minor form of tuberculosis.
- Marked pixels not lying in the range of high and low threshold are assigned as normal CXRs.
- The results of the algorithms are saved in the post processing step in the same folder for ease.

3.5 AUTOMATION OF SPUTUM SMEAR MICROSCOPY IMAGES

Automation for sputum smear microscopy images was done using MATLAB functions of image processing. The slides were taken from federal government services hospital, Islamabad and were ZN stained. ZN staining was preferred as it is cheaper and easily available as compared to Fluorescence staining that is more expensive. A bacilli segmentation algorithm is designed for detecting Acid fast bacilli and number of bacilli present in the image.

➢ PRE-PROCESSING

- The sputum smear slide images are taken as input in MATLAB.
- A mask was designed on the basis of color thresholding which will be used for extracting pixels information from the image.
- The information for thresholding was obtained from histogram.

➢ BACTERIAL SEGMENTATION AND EDGE DETECTION

- Acid fast bacilli can be detected by color, shape and size information. In this method we have identified AFBs on the basis of their color.
- RGB values of each pixel are extracted for comparison and the color band of the bacteria is measured according to the details given in the image. They usually vary depending on the image acquisition process and staining.
- A function create mask is used to generate the mask and a structuring element of 5*5 is defined which is then used for filtering.
- RGB values of each pixel are compared with bacteria's color band. Seed values are placed where color matches showing the presence of bacteria.
- For better visualization and observations of the detected spots dilation is done using square structuring element initialized earlier.
- Those objects which are 8-connected are returned using bwlabel function and then region props is used to measure properties of those connected components and placing a point at its centroid and a bounding box at its boundary.
- The detected AFB's are stored in an array which is then used in post processing step to detect count of bacilli.

➢ POST PROCESSING

- In the final step the length of the array is counted and the presence of even a single value in an array shows positive results. The output detects the positive image with the total number of bacilli present in an image.
- The absence of any value in the array will show the output as negative.

3.6 COMPARATIVE ANALYSIS OF DATA

All the results were analyzed statistically using SPSS version 18.0 software.

➢ TESTING PARAMETERS UNDER STUDY

Different parameters of patient's data were taken as variables for interpreting statistically. They includes Age group, gender, X-ray result, CXR Algorithm results, CXR algorithm outcome, Image types (Cavitation, Pleural effusion, Mediastinal hilar enlargement, milliary mottling, apical involvement, consolidations and air space infiltrates), microscopy results and outcome of microscopy algorithm.

➢ DATA FORMULATION

- The output results of the algorithm were inserted in the datasheet of standard data taken from hospital in Microsoft excel 2010.
- The formulated data is categorized into different variables.
- The transform command of PASW statistics version 18 was used to generate age groups from the data of patient age.
- The results of algorithm output that were in string data type was converted to numeric form for generating ROC curve using value label command and variable view.

➢ STATISTICAL DATA ANALYSIS

- The data is shown in three types of views in PASW statistics version 18 i.e. Data view, variable view and the output view.
- The main sheet on which working is done is the data view, the variables of data are edited and modified in variable view and the output of results is shown in output view.
- The cross tabulation command was used for finding the number of true positive, false positive, false negative, true negative.
- The standard data of patients CXR and microscopy results taken from hospital were cross tabulated against the results of algorithm data.
- Two different tables were generated that were for CXR and the other for microscopy specifying the number of true positive, false positive, false negative and true negative as shown in table 2 and table 3.

Table 2: Cross tabulation of CXRs data

	X-rays Positive	**X-rays Negative**
Algorithm X-rays Positive	True Positive	False Positive
Algorithm X-rays Negative	False Negative	True Negative

Table 3: Cross tabulation of Microscopy data

	Smear microscopy Positive	**Smear microscopy Negative**
Algorithm Smear microscopy images Positive	True Positive	False Positive
Algorithm Smear microscopy images Negative	False Negative	True Negative

- The presence of a condition that in our research is tuberculosis disease is called sensitivity. The sensitivity was measured by the formula mentioned in equation 3.1.[25]

$$Sensitivity = True\ positive/(True\ Positive + False\ Negative) \qquad (3.1)$$

- The absence of a condition that in our study is tuberculosis abnormality is called the specificity. The specificity was calculated using a formula shown in equation 3.2.[25]

$$Specificty = True\ Negative/(True\ negative + False\ positive) \qquad (3.2)$$

- The sensitivity and specificity values were used to obtain the maximum likelihood ratio. The positive likelihood for a condition was calculated using equation 3.3.[25]

$$Positive\ likelihood\ ratio = Sensitivity/1 - specificity \qquad (3.3)$$

- The negative likelihood ratio was calculated using equation 3.4.[25]

$$Negative\ likelihood\ ratio = 1 - Sensitivity/Specificty \qquad (3.4)$$

- Accuracy is the percentage or amount of correctly classified cases. The accuracy in our study is measured by the number of correctly detected images from the designed algorithm. The accuracy was calculated using equation 3.5.[13]

$$Accuracy = \frac{True\ Positive + True\ Negative}{(True\ Positive + True\ Negative + False\ Positive + False\ Negative)} * 100$$

- The Cross tabulation command was used for chi-Square testing.
- The ROC command was used to generate the ROC Curve for the designed algorithms.

3.7 COMPUTING TIME

- Computing time was also calculated for the designed algorithm. It is a time for processing one complete input. The execution of the algorithm and the time consume for detecting the abnormality was calculated using MATLAB component runtime 7.5.

CHAPTER 4: RESULTS

The CXR (chest x-ray radiographs) contain useful information for the interpretation of different abnormalities. Tuberculosis is examined on CXR's and it is also interpreted by the presence of acid fast bacilli in patient sample through different tests. One of the important tests is by examining the bacilli through Sputum smear microscopy. The images taken from digital microscope can be used for getting valuable information regarding the presence of bacilli. In this study the interpretation and analysis of results was done for the formulated data of CXR radiography and microscopy images.

4.1 AUTOMATED DETECTION OF TUBERCULOSIS USING WATERSHED SEGMENTATION APPROACH

The CXR images contain two dimensional representation of information about a three dimensional lung object for detecting tuberculosis. The important symptoms of tuberculosis identified in CXR's include pleural effusion, cavitation, consolidations, air space infiltrates, milliary mottling, apical involvement and mediastinal hilar enlargement.

Pleural effusion is an excess of fluid in the pleura and the chest cavity. The amount of lymphocytes usually increases in the fluid in case of tuberculosis disease. Pleural effusions are often referred to as water in the lungs (pleural cavity). [26] Cavitation is mainly caused in the upper lobes of the lungs because of the oxygen present in excess amount. The bacilli remain alive in this region due to excess oxygen present and causes pus formation which rupture to yield inflammation. The tissues of the lungs are mainly damage due to cavitation formation. [27] The air space infiltrations are divided into two types that include milliary mottling and consolidations. The milliary mottling indications are shown as hazy shadows. However, consolidations are rather circular and present in the form of larger isolated opacities. These features were identified in CXRs in the form of small nodules either present in the lungs or at the boundaries of the lungs.

Apical involvement is the presence of tuberculosis in the apex of the lung. The apex is the region where high amount of oxygen tension gradient is established. The apex region is occupied by bacteria and the infection caused by bacteria results in the formation of consolidations. This results in stretches or bends in the clavicle or apex region of the lung. The mediastinal hilar enlargement is an abnormal enlargement of the hilar of the mediastinum. The enlargement occurs in case of severe damage to the hilar tissue and can lead to the formation of tumors. The features are taken as data variables for comparison of CXR algorithm results with reference standard CXR data of the patients. Our algorithm is detecting tuberculosis in CXRs on the basis of rate of abnormality present. The results differentiate major and minor TB cases from normal cases. The major tuberculosis is detected as the one in which three or more than three abnormalities are present. The minor tuberculosis includes the one in which two abnormalities are confirmed. However the images showing least chances of abnormalities are shown as negative.

In figure 3(a) a sample CXR image of a female is shown. From the reference standard data the results shows the presence of mediastinal hilar enlargement, apical involvement and pleural effusions. Some of the right lung region is also showing the symptoms of consolidations and milliary mottling. The algorithm detected this image as major type of tuberculosis which was according to the reference data. The output of the algorithm results are shown in figure 3(b). In figure 4(a) another CXR image of a female is shown. The symptoms of mediastinal hilar enlargement, scars on both lungs and small infiltrates on right lung were present. The output of the algorithm is shown in figure 4(b) showing major form of tuberculosis. In figure 5(a) a CXR of a female is shown. The figure indicates that there are confirmed chances of apical region involvement and mediastinal hilar enlargement. The output is shown in figure 5(b) indicating the image as minor tuberculosis case. Similarly, another example is shown in figure 6(a) in which there is infection in tracheal boundaries region and apex. The CXR is showing mediastinal hilar enlargement and

tuberculosis in apex region. There are some scars present on both the lungs but they are not confirmed indication of tuberculosis. They are actually clear representation of blood vessels and other tissues of the lungs and the algorithm output is shown in figure 6(b). Our designed system has also detected normal images. The normal images are the one with least chances of the disease as shown in figure 7(a) and 8(a). There are some regions in figure 7(a) representing disease in the left lung but they are not confirmed. It is possible that these minor indications represented in the CXR are the tissues or some other sort of other disease e.g. pneumonia, heart related disease, tumor but are not confirmed indication for tuberculosis. The output from the algorithm is shown in figure 7(b) and 8(b) for normal images. The algorithm is detecting tuberculosis on the basis of pixels information of the lung object. Watershed segmentation iteratively scans the whole lung region and identifies those regions showing abnormality through a scanning window of fixed size. The threshold values are set which can help out in extracting the required information from the images.

4.2 AUTOMATED DETECTION OF TUBERCULOSIS USING SMEAR MICROSCOPY IMAGES

The second part of our research was bacilli segmentation using Smear microscopy images. The mycobacterium tuberculosis bacilli can be identified on the basis of features i.e. shape, color and size information. We have taken color feature into consideration for identifying Acid fast bacilli in microscopy images. The staining techniques for identifying bacilli on the basis of color include ZN and fluorescence staining. In ZN staining the bacilli appeared as pink and in fluorescence staining they appears yellowish and green. We have chosen ZN staining because of convenience and cost effectiveness. The positive slide images from the dataset are taken in figure 9(a), 10(a) and 11(a). The algorithm results with bacilli count are shown in figure 9(b), 10(b) and 11(b). The negative images from the dataset are taken in figure 12(a) and 13(a). The output of negative images is shown

in figure 12(b) and 13(b). The identification of bacilli is done on the basis of color thresholding. After identifying bacilli the number of bacilli is counted by the system designed.

Figure 3(a): This figure shows original image showing pulmonary regions of human body. This is a CXR of a female gender.

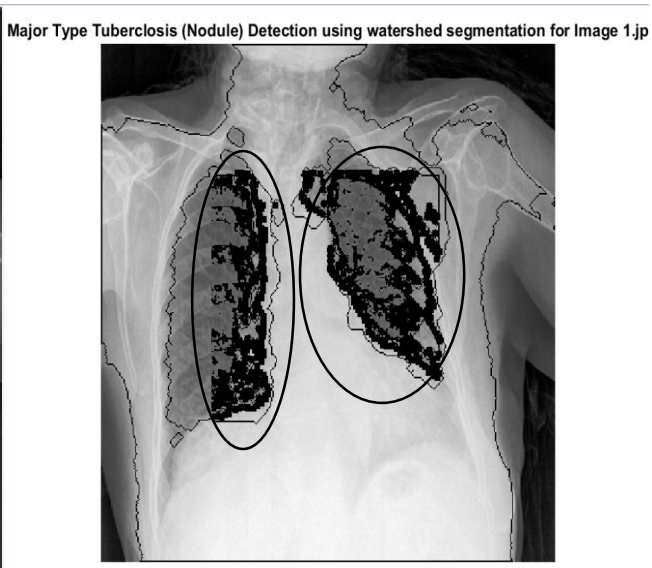

Figure 3(b): This figure shows result for figure 3(a) indicating abnormality. The regions in black indicate the major type of tuberculosis.

Figure 4(a): This figure shows original image showing pulmonary regions of human body. This is a CXR of a female gender.

Figure 4(b): This figure shows result for figure 4(a) indicating abnormality. The regions in black indicate the major type of tuberculosis.

Figure 5(a): This figure shows original image showing pulmonary regions of human body. This is a CXR of a female gender.

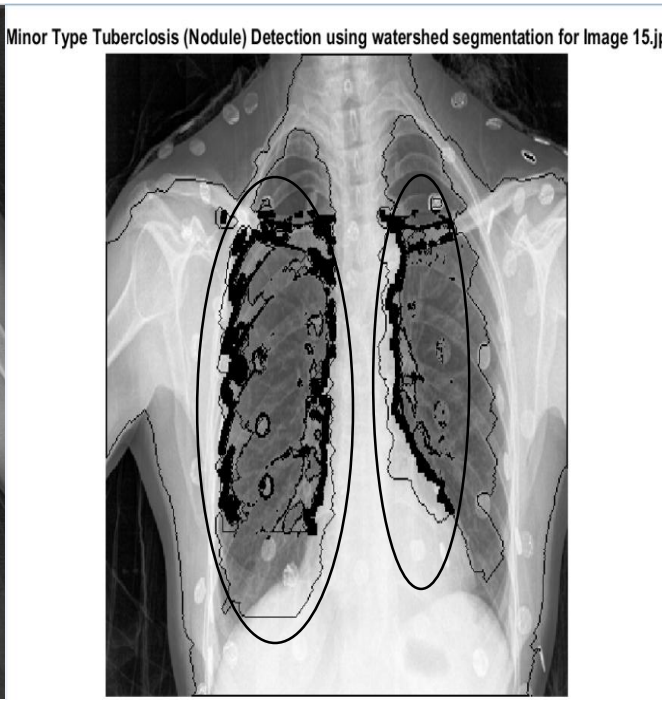

Figure 5(b): This figure shows result for figure 5(a) indicating abnormality. The regions in black indicate the minor type of tuberculosis.

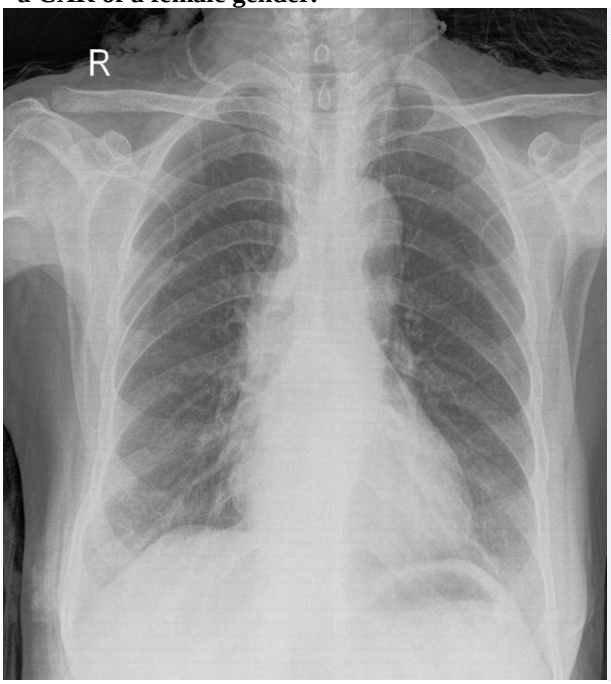

Figure 6(a): This figure shows original image showing pulmonary regions of human body. This is a CXR of a female gender.

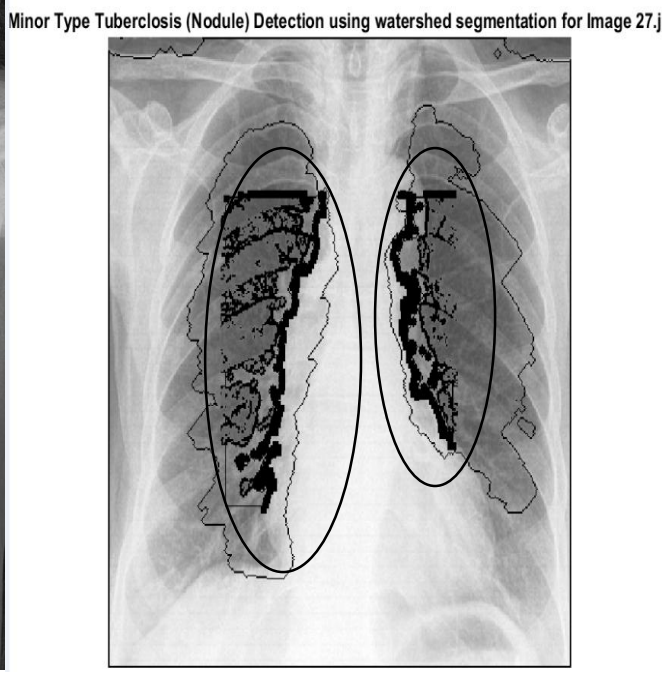

Figure 6(b): This figure shows result for figure 6(a) indicating abnormality. The regions in black indicate the minor type of tuberculosis.

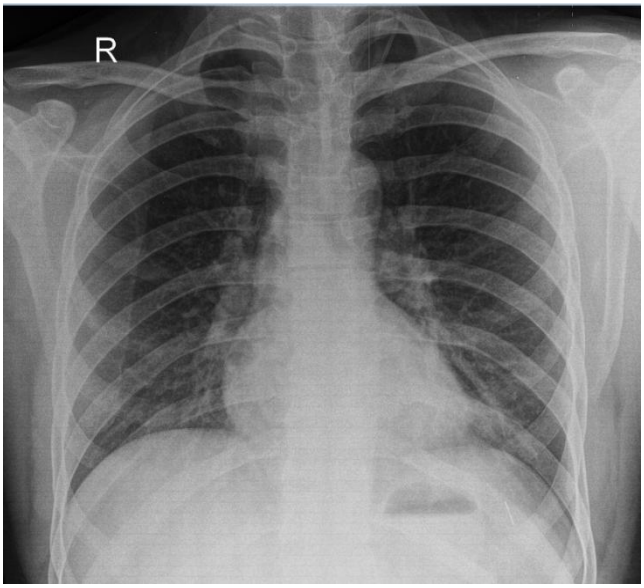

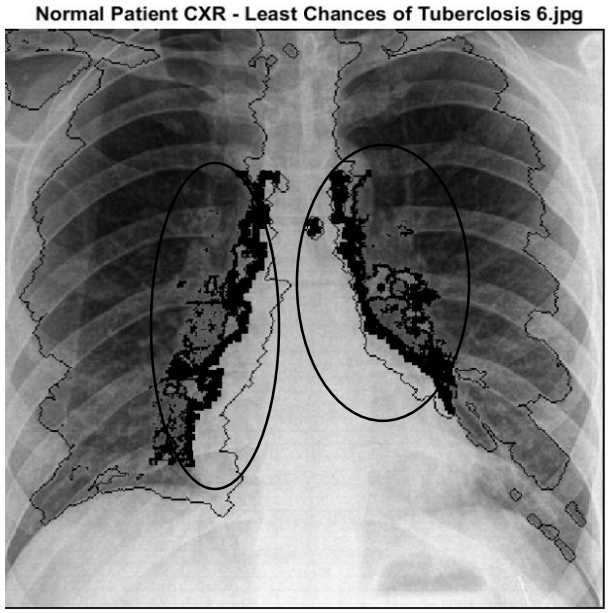

Figure 7(a): This figure shows original image showing pulmonary regions of human body. This is a CXR of a male gender.

Figure 7(b): This figure shows result for figure 7(a).The black color in figure shows that the CXR contained least chances for the presence of a disease.

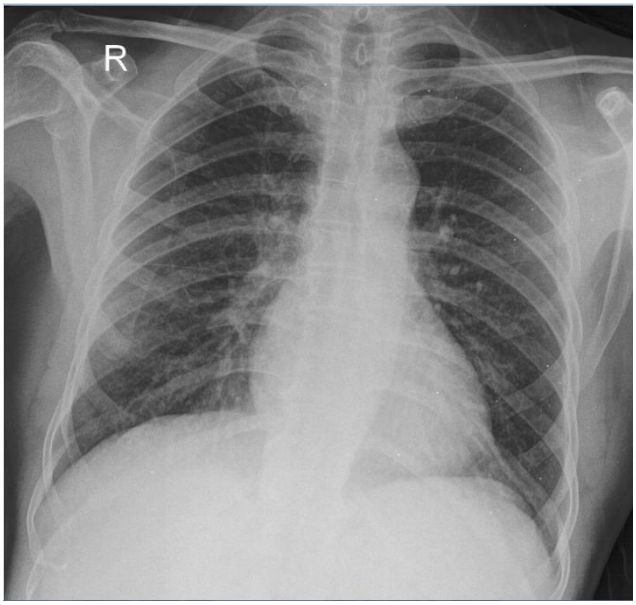

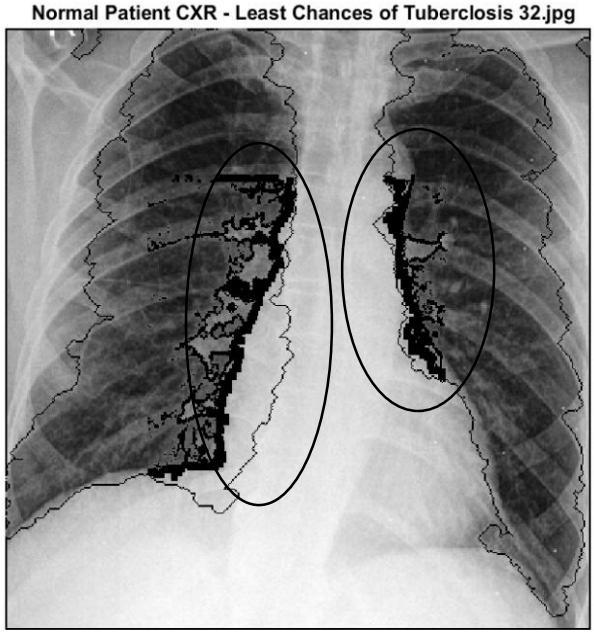

Figure 8(a): This figure shows original image showing pulmonary regions of human body. This is a CXR of a male gender.

Figure 8(b): This figure shows result for figure 8(a).The black color in figure shows that the CXR contained least chances for the presence of a disease.

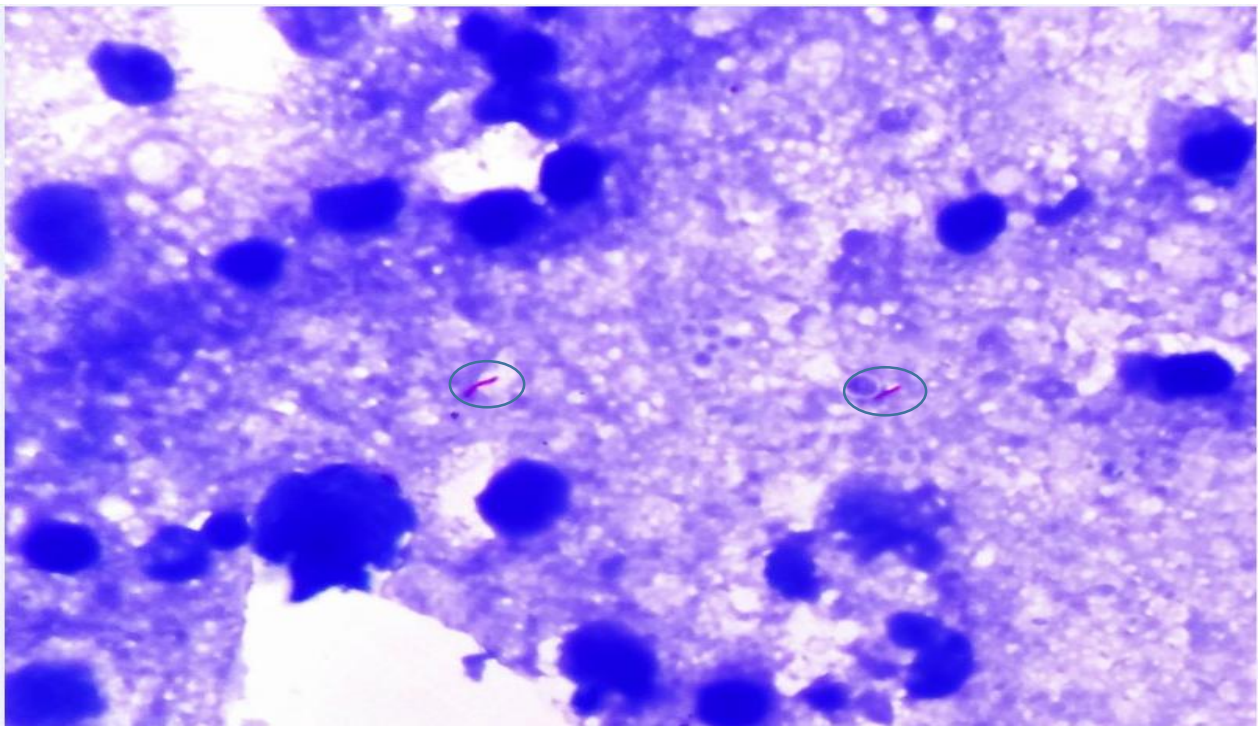

Figure 9(a): This figure shows original image showing AFB's in pink color with ZN staining in blue background.

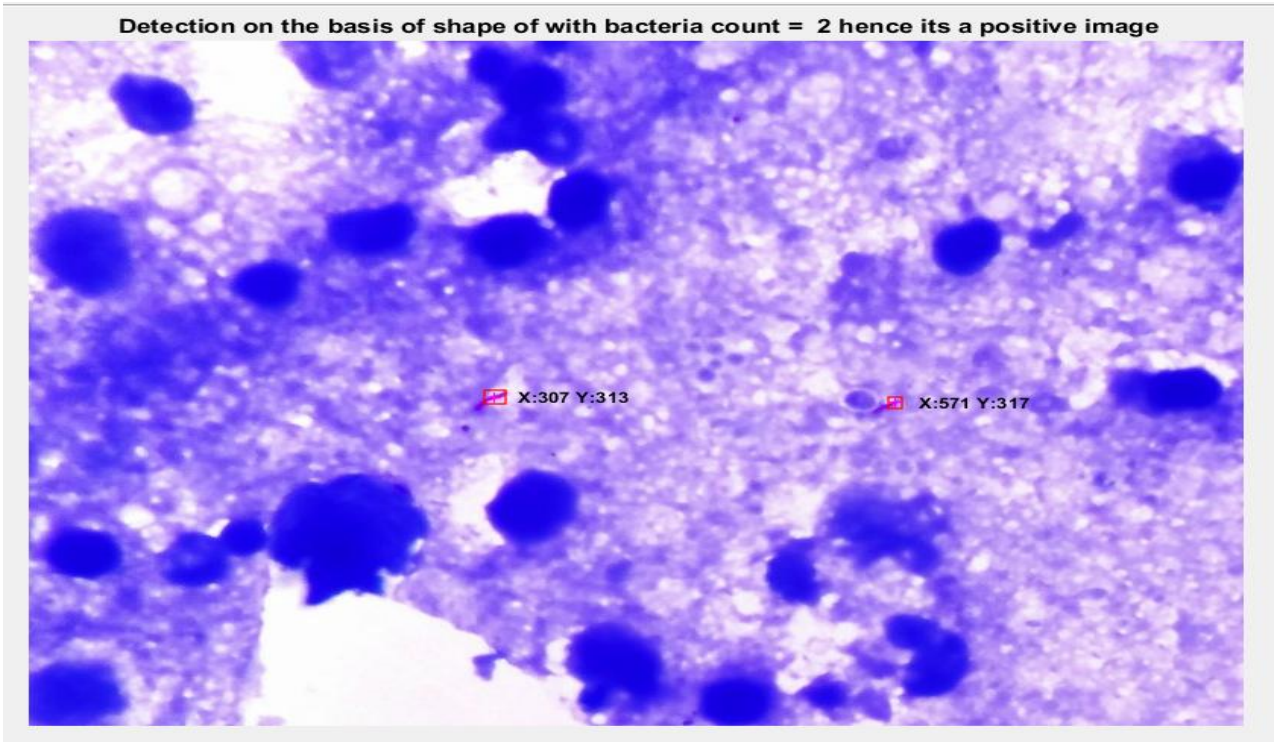

Figure 9(b): This figure shows result for figure 9(a). AFB's are identified by pink color box and number of AFB's counted by number of boxes are shown in the output as two AFB's.

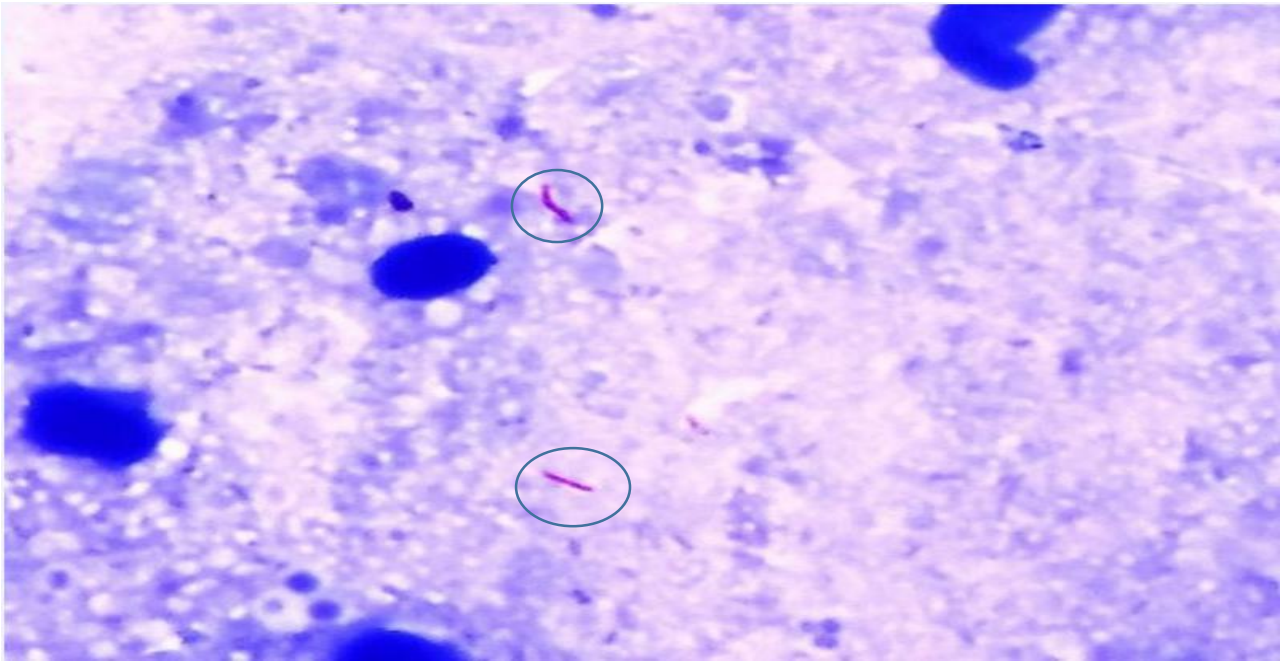

Figure 10(a): This figure shows original image Showing AFB's in pink color with ZN staining in blue background.

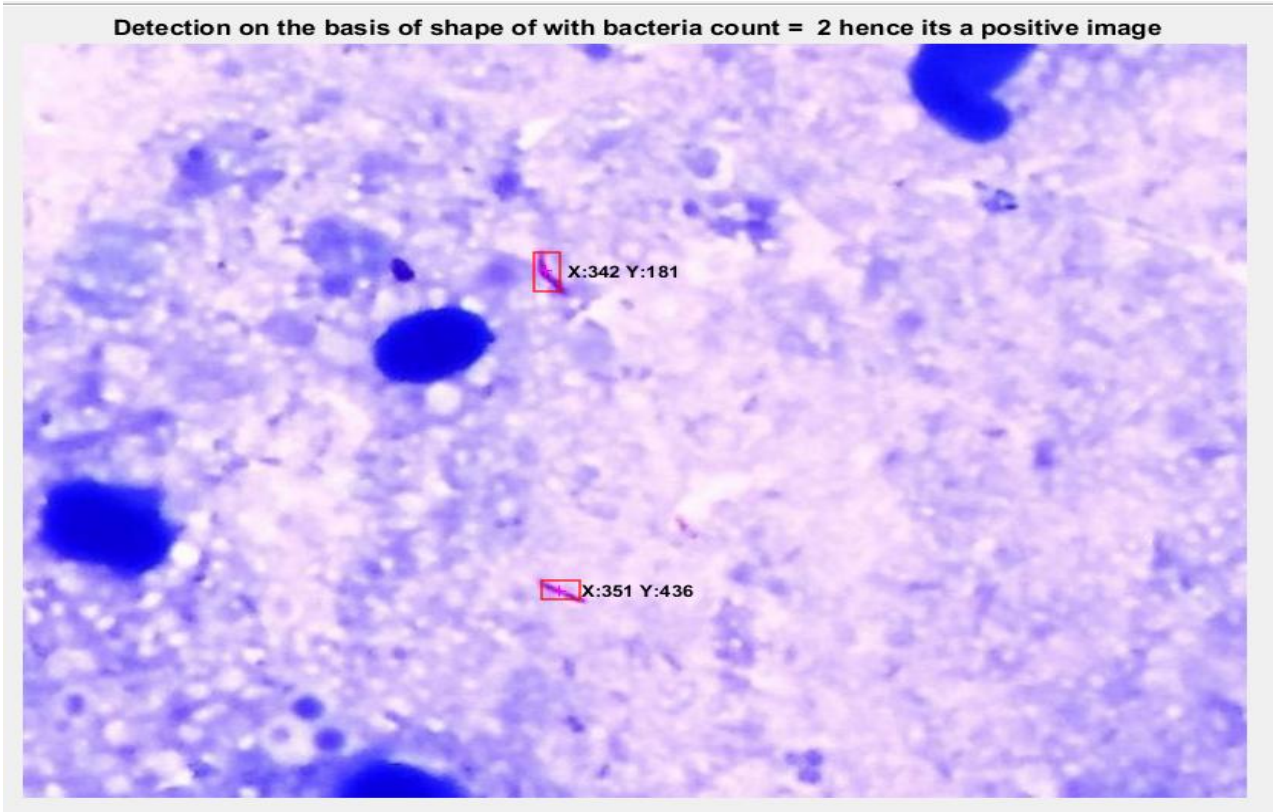

Figure 10(b): This figure shows result for figure 10(a). AFB's are identified by pink color box and number of AFB's counted by number of boxes are shown in the output as two AFB's.

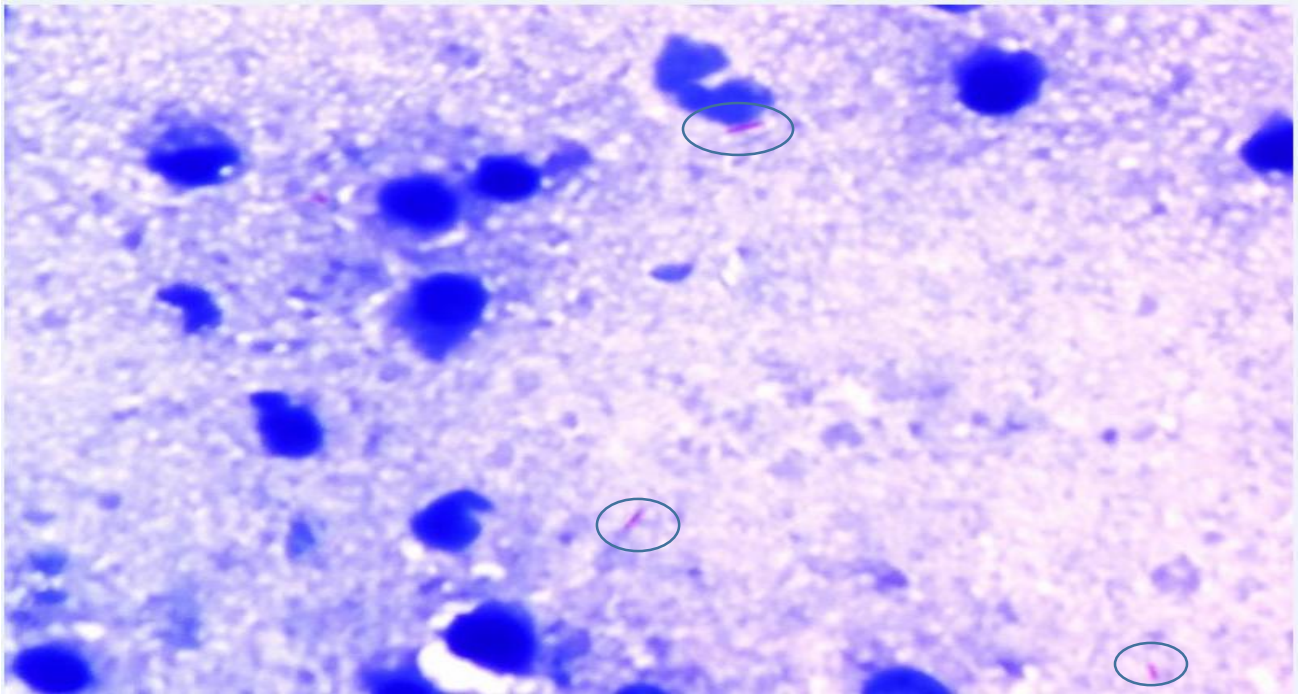

Figure 11(a): This figure shows original image Showing AFB's in pink color with ZN staining in blue background.

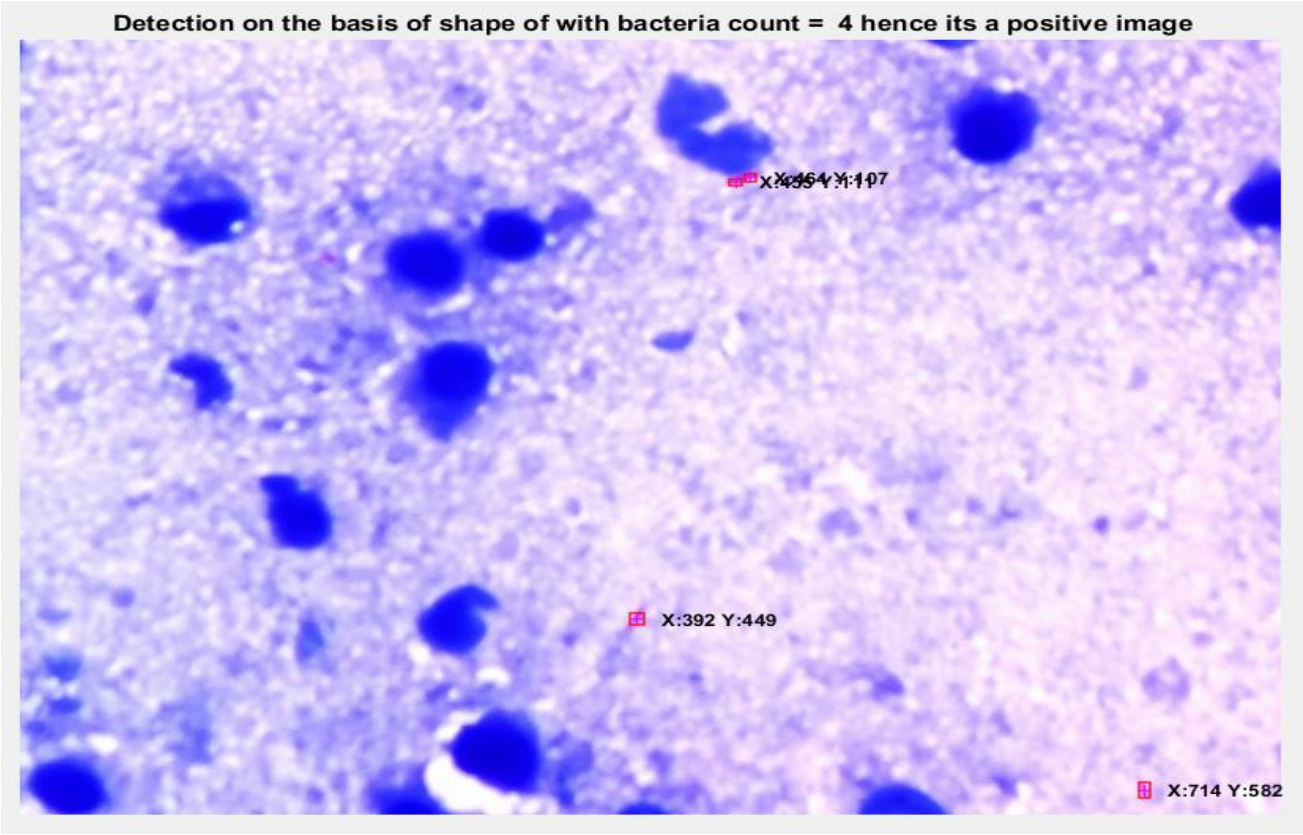

Figure 11(b): This figure shows result for figure 11(a). AFB's are identified by pink color box and number of AFB's counted by number of boxes are shown in the output as four AFB's.

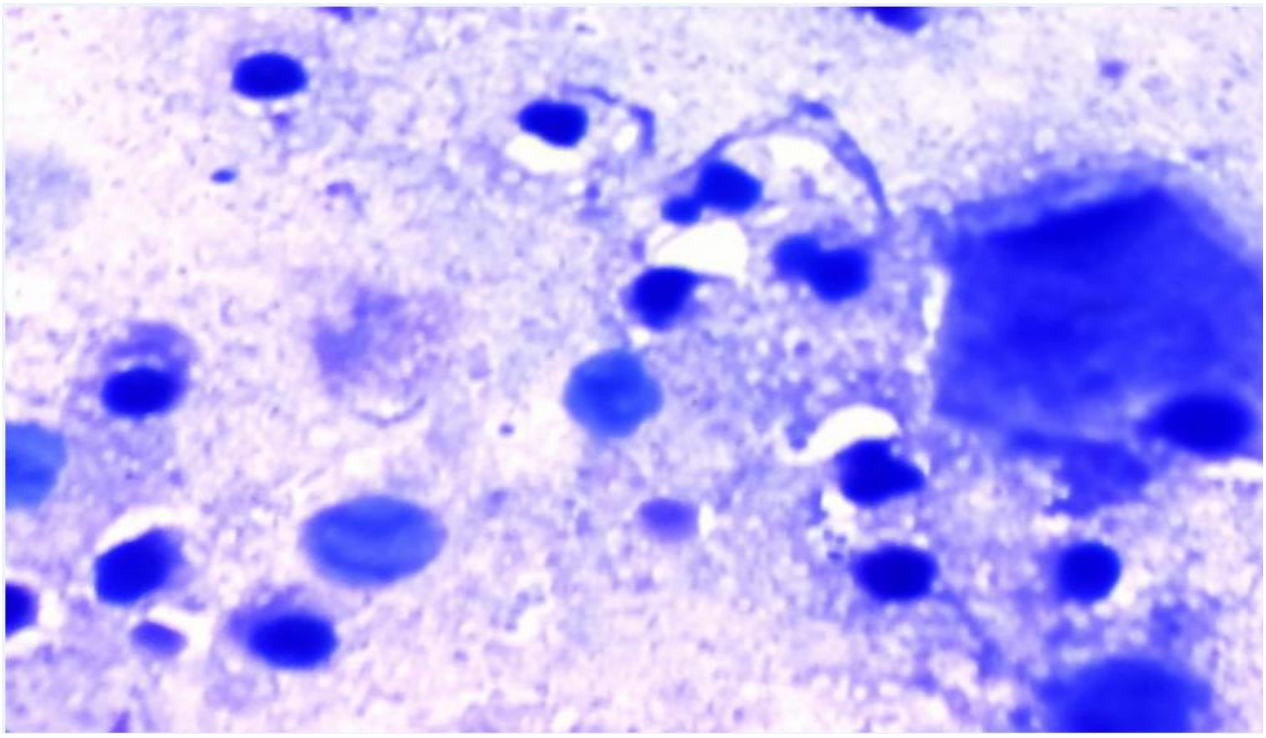

Figure 12(a): This figure shows original image with ZN staining in blue background.

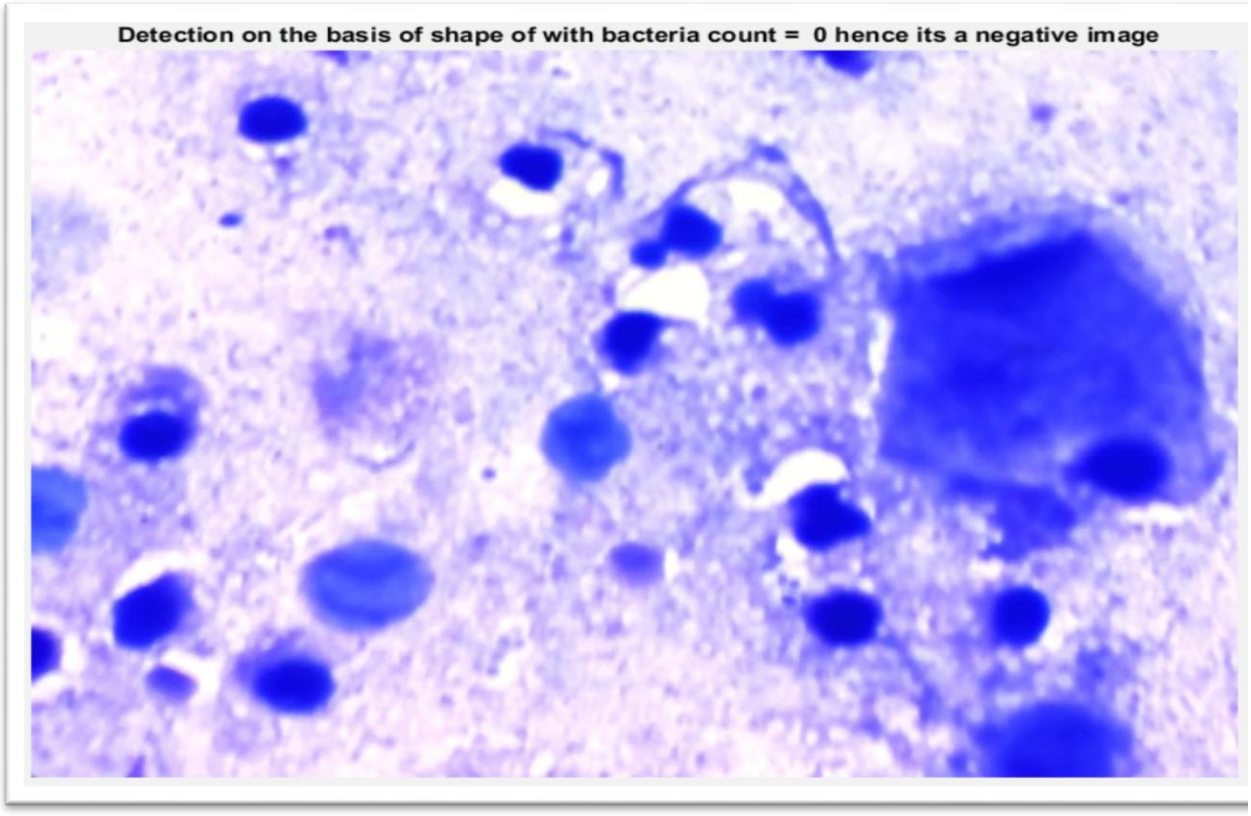

Figure 12(b): This figure shows result for figure 12(a). No AFB's are identified showing the image result as negative.

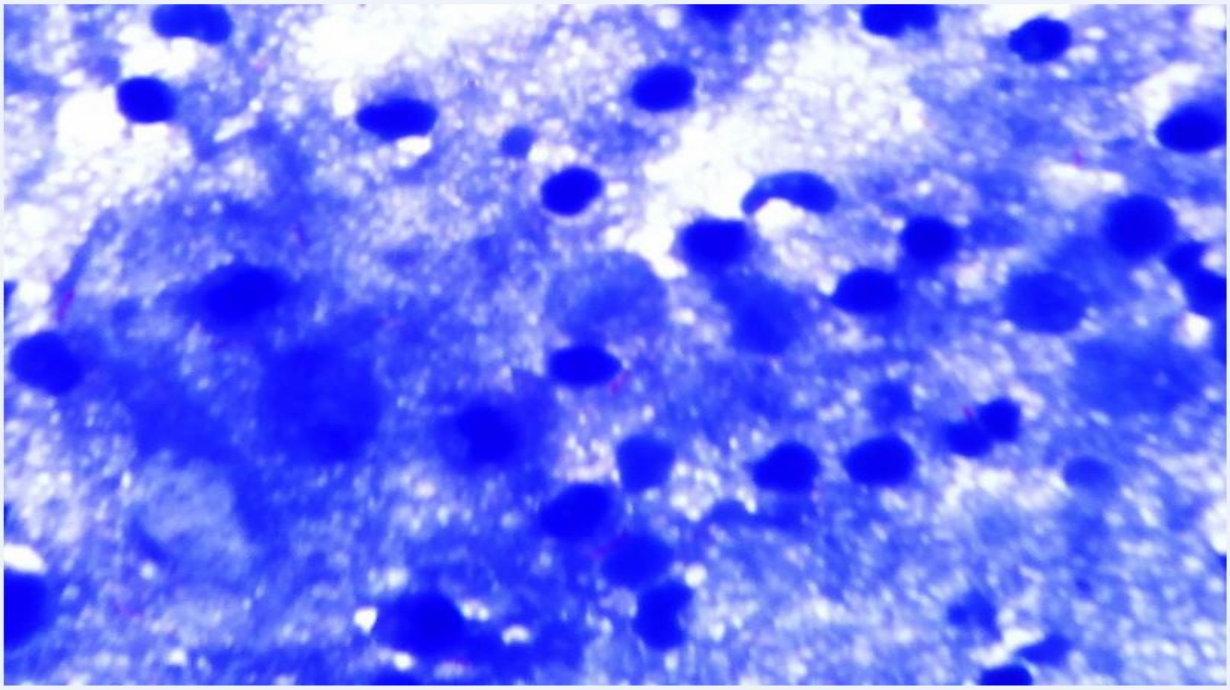

Figure 13(a): This figure shows original Image with ZN staining in blue background.

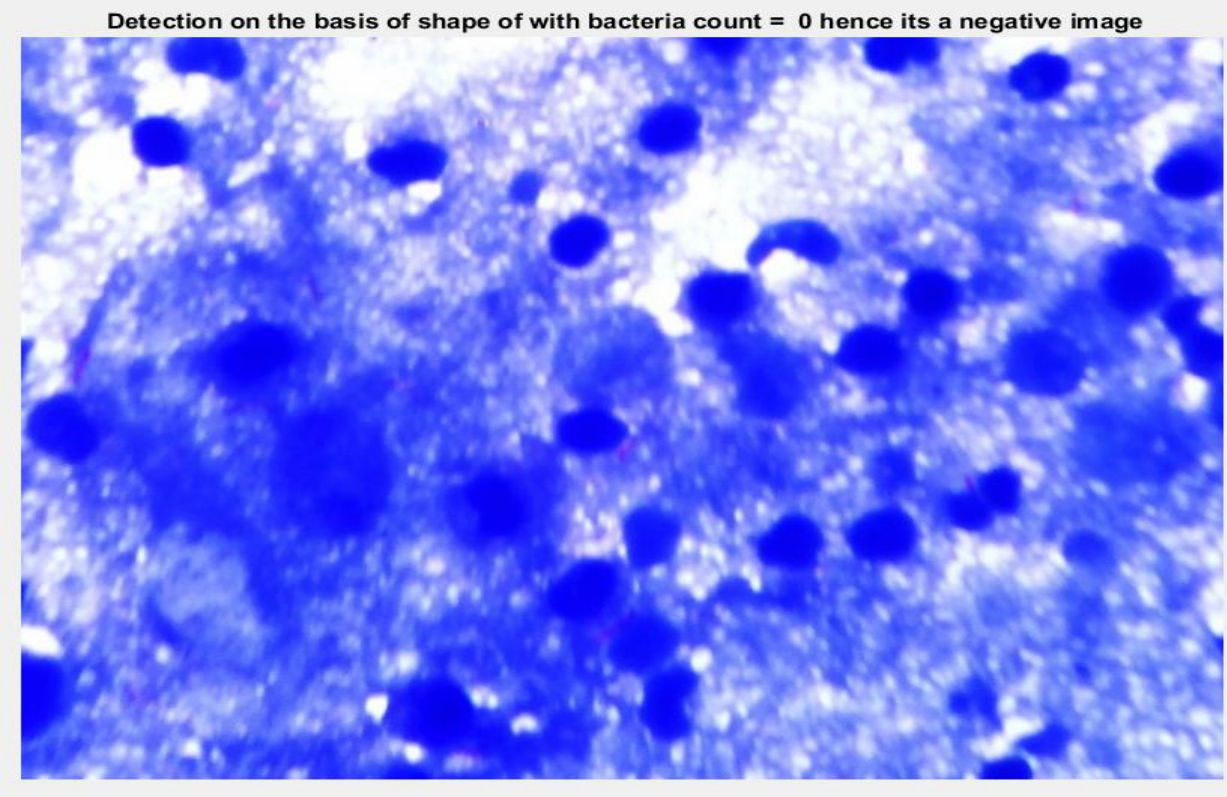

Figure 13(b): This figure shows result for figure 13(a). No AFB's are identified showing the image result as negative.

4.3 ANALYSIS OF DATA

The third part of this research study was to analyze the data using PASW statistics 18. The data taken from hospital contains 10 normal and 40 abnormal CXRs as shown in figure 14(a). The data for microscopy contains 24 negative and 26 positive sputum smear slides as shown in figure 14(b). The results of algorithms are compared with reference standard data. The number of true positives, true negatives, false positives and false negative are represented graphically with age group variable for Chest radiograph in figure 15. Similarly, the microscopy results with age group are represented graphically in figure 16. Similarly, the variable gender is also taken with our results for Chest radiographs in figure 17 and for smear microscopy in figure 18. The number of true positives, true negatives, false positives and false negatives are shown in table 4 for chest radiography and in table 5 for smear microscopy. This information is used to calculate sensitivity from equation 3.1 and specificity from equation 3.2 for the designed algorithms. The sensitivity of 98% and specificity of 70% was obtained for CXR tuberculosis detection algorithm. The positive likelihood ratio of 3.26 was obtained and the negative likelihood ratio of 0.03 was obtained for CXR tuberculosis detection system using equation 3.3 and 3.4. The accuracy of 92% was obtained for chest radiograph images using equation 3.5. The sensitivity of 92% and the specificity of 96% were obtained for bacilli segmentation algorithm. The positive likelihood ratio of 23 and negative likelihood ratio of 0.08 was obtained for bacilli segmentation algorithm. The accuracy of 94% was obtained for bacilli detection system. The association and dependence of the standard testing method and the designed algorithms was checked using Pearson Chi-square test. The p value of less than 0.05 was obtained for the two algorithms as shown in table 6. This shows that there is no association between the proposed systems and the standard reference systems. The receiver operator curve (ROC) was generated that represents the accuracy of the designed algorithms. Area under the curve is the region

for finding the accuracy of the any system. The area under the curve of 0.838 was obtained for chest radiography tuberculosis detection algorithm as shown in figure 19. The sensitivity of 0.975 and specificity of 0.3 was taken as cut off point for detecting the abnormality correctly. The value above or below this cutoff value will detect either sensitivity or specificity correctly. The cut off value is the point for obtaining the desired sensitivity or specificity of the algorithm. The area under the curve of 0.941 was obtained for bacilli detection algorithm and cut off point was set at the sensitivity of 0.923 and specificity of 0.042. In figure 20 the ROC for bacilli detection algorithm is shown. The execution time for the two algorithms was calculated using MATLAB command (Run and Time) for checking the speed. The profile time indicates the total time for execution of algorithm. Execution time for CXR abnormality detection algorithm was 564 Seconds for 50 CXRs sample images. However, time for microscopy bacilli detection algorithm was 100 seconds for 50 sputum sample images.

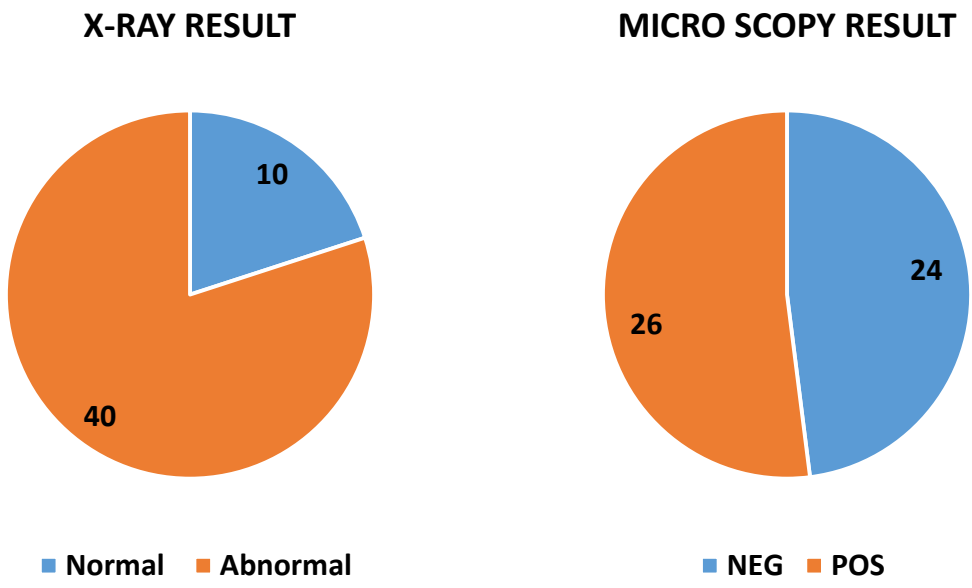

Figure 14(a): This figure shows reference standard data for chest radiographs. The number of abnormal individuals with abnormal x-ray are more as compared to normal, Figure 14(b): This figure shows reference standard data for smear microscopy. The number of positive slide images are more than negative images.

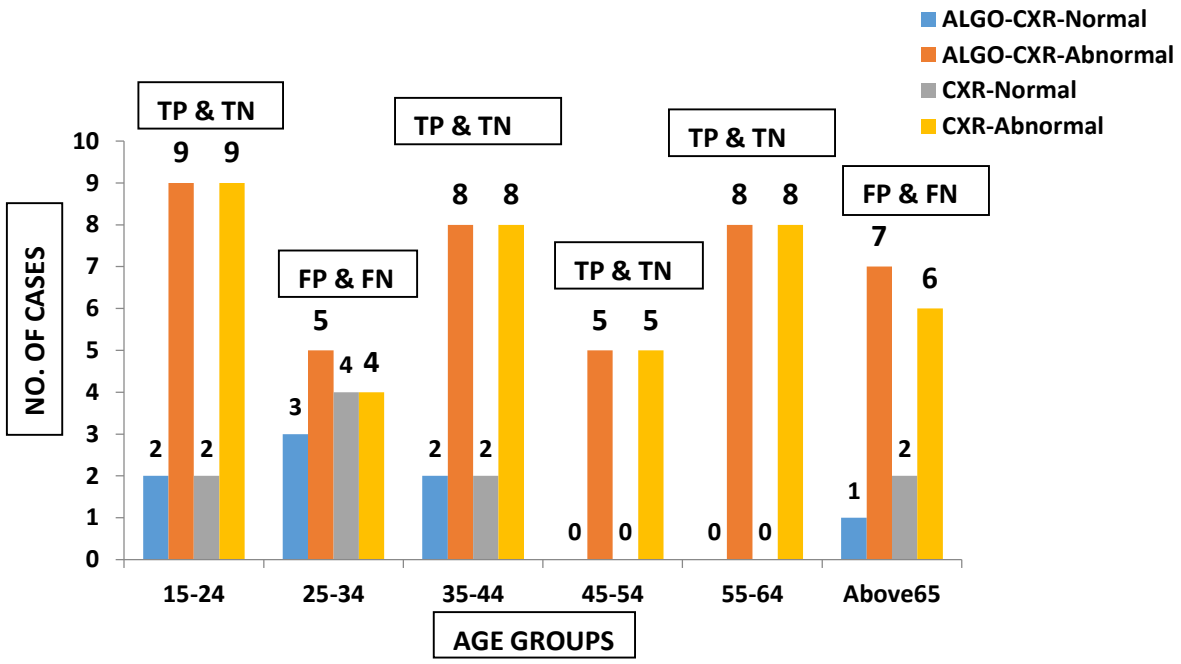

Figure 15: This figure shows graphical representation of reference standard data and algorithm data along with age group for chest radiography. The constant bars are representing true positive and true negatives. However fluctuations in bars represents false positive and false negatives.

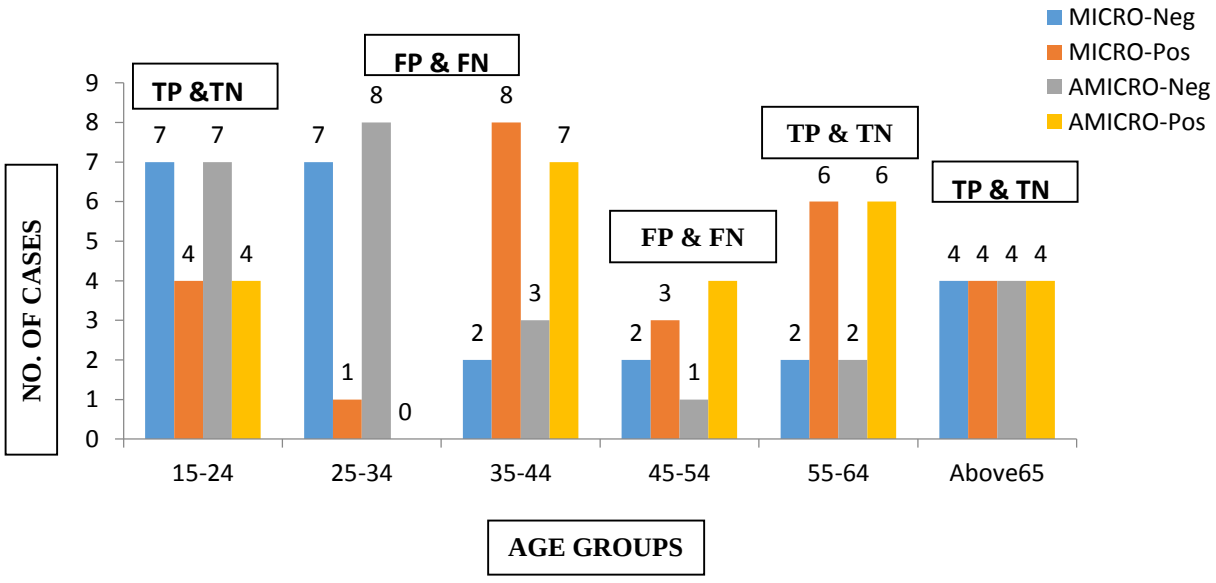

Figure 16: This figure shows graphical representation of reference standard data and algorithm data along with age group for sputum smear microscopy. The constant bars are representing true positive and true negatives. However fluctuations in bars represents false positive and false negatives.

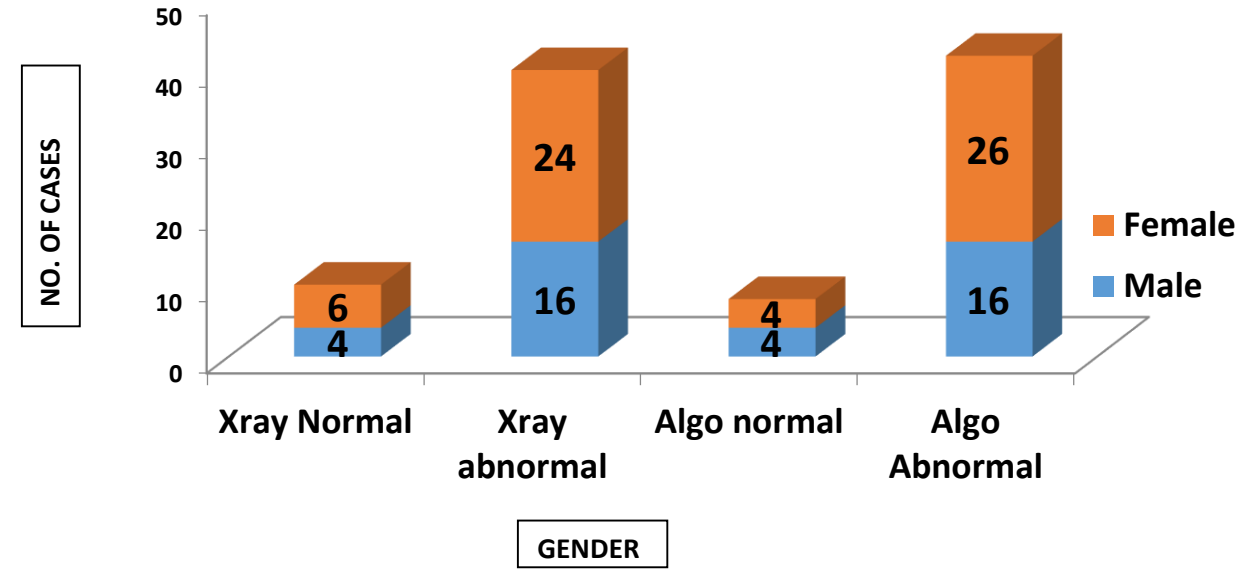

Figure 17: This figure shows graphical representation of reference standard data and algorithm data along with gender for chest radiography. In the given dataset the number of females suffering from tuberculosis are greater as compared to male gender.

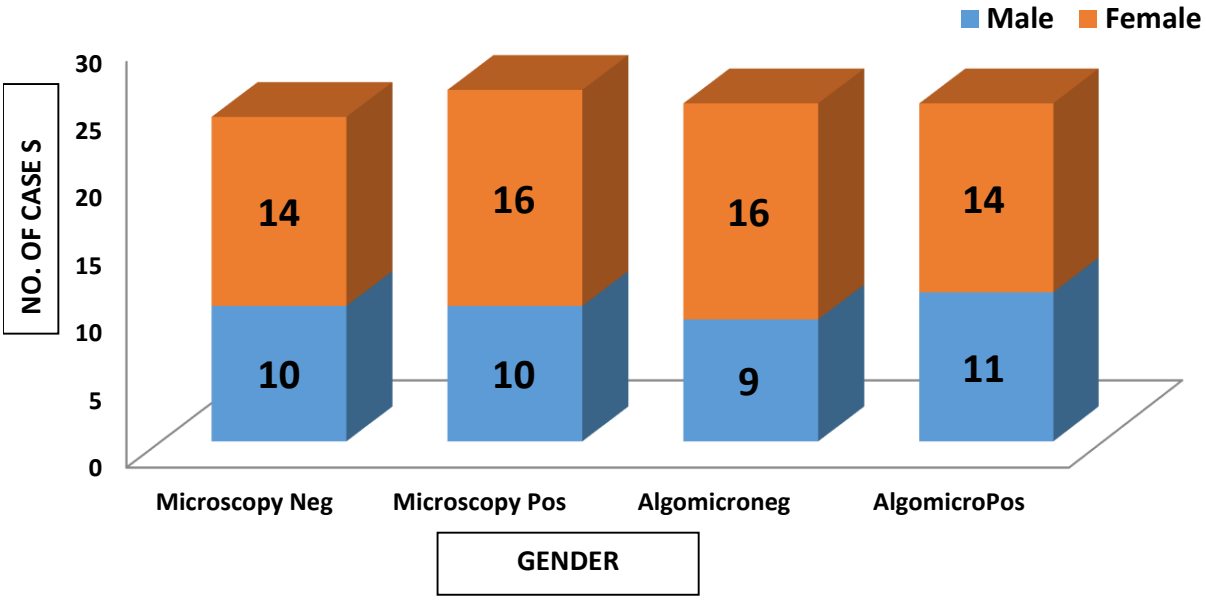

Figure 18: This figure shows graphical representation of reference standard data and proposed algorithm data along with gender for smear microscopy. In the given dataset the number of females suffering from tuberculosis are greater as compared to male gender.

Table 4: Tabular representation of true positives, false positives, false negatives and true negatives for Chest radiography.

	X-rays Positive	X-rays Negative
Algorithm X-rays Positive	39(TP)	3(FP)
Algorithm X-rays Negative	1(FN)	7(TN)

Table 5: Tabular representation of true positives, false positives, false negatives and true negatives for Smear microscopy.

	Smear microscopy Positive	Smear microscopy Negative
Algorithm Smear microscopy Positive	23(TP)	1(FP)
Algorithm Smear microscopy Negative	2(FN)	24(TN)

Table 6: Pearson Chi-Square test results for chest radiography and bacilli segmentation. The sig. value of lesser than 0.05 was obtained for both the proposed algorithms and it shows the independence of laboratory based system from our proposed algorithm system.

Test Type	Value	Df	Sig.	Remarks
Pearson Chi-Square (X-rays	27.121[a]	1	.000	As the p =.000 which is less than the 0.05 (p<0.05) which indicates that there is significant difference/ no association between the two techniques of CXRs
Pearson Chi-Square (Microscopy	38.782[a]	1	.000	As the p =.000 which is less than the 0.05 (p<0.05) which indicates that there is significant difference/ no association between the two techniques of Microscopy
N	50			

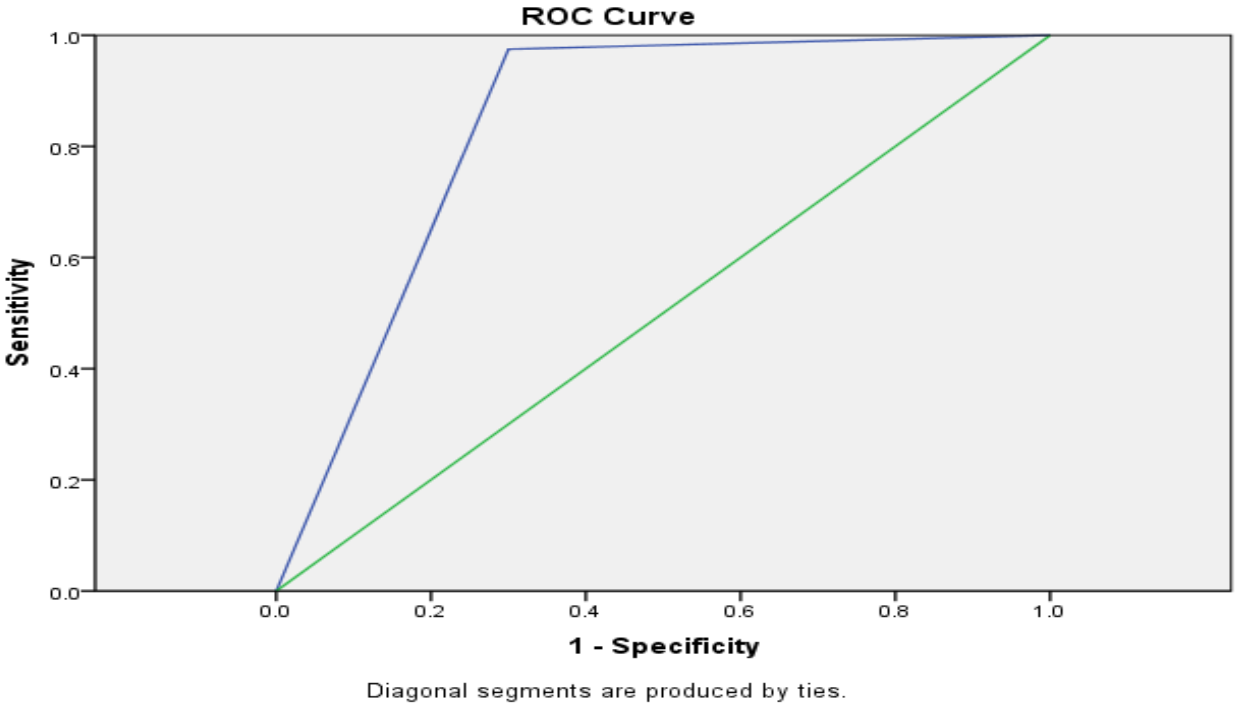

Figure 19: This figure shows ROC interpretation for chest radiography algorithm. The null hypothesis is shown by green and alternative hypothesis is shown by blue lines. The blue lines generated rejected the null hypothesis and area under the curve shows accuracy of the proposed algorithm.

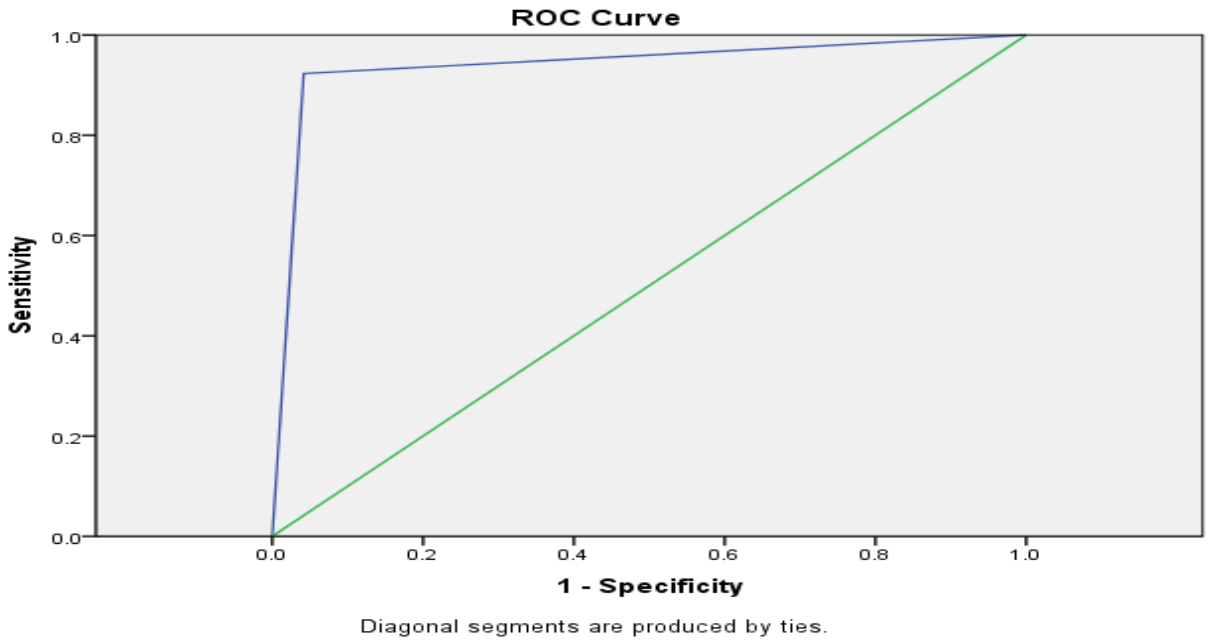

Figure 20: This figure shows ROC interpretation for bacilli segmentation algorithm. The null hypothesis is shown by green and alternative hypothesis is shown by blue lines. The blue lines generated rejected the null hypothesis and area under the curve shows accuracy of the proposed algorithm.

CHAPTER 5: DISCUSSION

Medical image processing is used for automating different medical procedures for the treatment and diagnosis of diseases. In this research the techniques of medical image processing were implemented for screening of tuberculosis patients. The screening procedure comprises of two algorithms that were chest radiography algorithm and tuberculosis bacilli detection algorithm. Watershed segmentation approach was followed for chest radiography algorithm from the work done earlier and lungs were isolated for identifying tuberculosis. [30] However in the previous research no such accuracy was mentioned. Previous work was done for other abnormalities of the lungs regions too. Our proposed system would focus on tuberculosis and had shown reliability of use with accuracy of 92% which is greater than other algorithms designed. [29]

Bacilli segmentation system was designed using color thresholding approach and already proposed research work [21] was taken into consideration for designing the system. However 94% accuracy was obtained as compared to already designed K-means clustering and Otsu thresholding approach which had shown accuracy of above 98%. Further work for our designed bacilli segmentation algorithm is needed in future to obtain accuracy above 98% by taking all the three main parameters i.e. size, shape and color. However our proposed bacilli segmentation has performed best as compared to other systems proposed earlier with accuracy lesser than 94%. [29]

Different variables from reference standard data were compared with algorithms results. Interpretation of algorithm was compared with reference standard technique results. The numbers of true positive and true negative are greater than false positive and false negative so our designed algorithm is accurate in detecting tuberculosis. The sensitivity and specificity is calculated for checking the usefulness and correct testing by the algorithms. Sensitivity of chest radiography algorithm was greater than bacilli segmentation algorithm. However, the specificity of bacilli

segmentation algorithm was greater as compared to chest radiography algorithm. The positive likelihood ratio indicates bacilli segmentation algorithm is more useful as compared to chest radiography algorithm. The positive likelihood of greater than one indicates correct results. Similarly, the negative likelihood ratio of less than one is good. Values of negative likelihood also indicate the bacilli segmentation algorithm can correctly help in diagnosis of the disease. The accuracy of bacilli segmentation algorithm was greater. Pearson Chi-Square test interpretations shows that there is no association between the designed algorithm and standard reference techniques available. The P-value of less than 0.05 was obtained which shows that the techniques are independent of each other and the null hypothesis was rejected. According to null hypothesis the techniques are dependent on one another. However, the alternative hypothesis suggests that they are independent of each other. The alternative hypothesis was accepted for chest radiography algorithm and bacilli segmentation algorithm. The receiver operator curve was interpreted for the algorithms for analyzing the accuracy. According to null hypothesis no sensitivity or specificity will be obtained where Ho will be equal to 0.5. The null hypothesis was rejected and the area under the curve of 0.838 was obtained for chest radiography algorithm and 0.941 for bacilli segmentation algorithm. The cut off value was calculated for obtaining the accuracy at which both sensitivity and specificity will be good. The cutoff points are discussed earlier in results section 4.3. The area under the curve of bacilli segmentation algorithm was greater and the accuracy will be greater. The computing time of bacilli segmentation algorithm was less as they contain less information for processing as compared to chest X-rays containing large amount of pixel information for interpretation. Hence, the computational time of chest radiography algorithm is greater. The proposed algorithm will be used by the radiologists in hospital and microbiologists in laboratories for identifying the disease. The reports generated will be used by doctors and medical specialists in diagnosis and treatment of the disease. However there are some limitations to the proposed system.

The proposed bacilli detection algorithm can identify AFB's on the basis of color so it can only be used with slides that are ZN stained and give pink color to AFB's. Similarly when we are capturing information from 3D to 2D much of the information is lost in this process so the results should be interpreted on the basis of both of the proposed algorithms. Moreover, the specificity of chest radiography algorithm is less which shows that there are chances that our algorithm will detect diseases other than tuberculosis in the lungs at the time of execution.

CHAPTER 6: CONCLUSION & RECOMENDATIONS

Bacilli segmentation proposed algorithm was found to be better for screening of tuberculosis patients because its achieved specificity and accuracy were greater along with large positive likelihood ratio and small negative likelihood ratio. The sensitivity in bacilli segmentation algorithm is basically due to the presence of acid fast bacilli and specificity is the correct identification of bacilli. The specificity of bacilli detection algorithm is more accurate in identifying the AFB's in images. Due to these reasons bacilli segmentation algorithm is expected to reduce human error and fatigue in manual TB detection. Also because of the same reason bacilli segmentation algorithm is expected to make the screening procedure more robust. The severity of the disease could also be judged through bacilli segmentation techniques by counting number of segmented bacilli. The greater the number of bacilli more will be the chances of severity of the disease. On the other hand in chest radiography algorithm, sensitivity is the presence of abnormality in lungs. Chest radiography algorithm had higher sensitivity and therefore would assist in differentiating between minor and major tuberculosis. For chest radiography algorithm the computation time is more but it could reduce human fatigue by processing all the images available iteratively automatically. However, the confirmation of the presence of the disease is not much clear from one type of test. Therefore, different types of tests are performed for reliable TB identification. It will be very best, to use both the proposed algorithms simultaneously for diagnosis and treatment of tuberculosis with very high reliability.

Recommendations for Future Work

- For the proposed bacilli detection system can identify AFB's on the basis of staining color. The shape and size information could also be taken into consideration for detecting AFB's that would overcome the limitation of staining.
- For chest radiograph detection system more features of lungs should be taken into consideration which can detect abnormalities other than tuberculosis e.g. cancer, heart diseases and pneumonia.
- The proposed systems should be modified in such a way that only a single input would give an indication for the presence of tuberculosis abnormality and bacilli detection. This can be done using carbon filters. Combining both the proposed algorithms would reduce execution time.

REFERENCES

[1] A. A. Velayati and P. Farnia, "Morphological Characterization of Mycobacterium tuberculosis," in Understanding Tuberculosis-Deciphering the Secret Life of the Bacilli, ed: InTech, 2012.

[2] B. Van Ginneken, S. Katsuragawa, B. M. ter Haar Romeny, K. Doi, and M. A. Viergever, "Automatic detection of abnormalities in chest radiographs using local texture analysis," IEEE transactions on medical imaging, vol. 21, pp. 139-149, 2002.

[3] T. Xu, I. Cheng, R. Long, and M. Mandal, "Novel coarse-to-fine dual scale technique for tuberculosis cavity detection in chest radiographs," EURASIP Journal on Image and Video Processing, vol. 2013, p. 3, 2013.

[4] P. Maduskar, L. Hogeweg, R. Philipsen, S. Schalekamp, and B. van Ginneken, "Improved texture analysis for automatic detection of tuberculosis (TB) on chest radiographs with bone suppression images," in SPIE Medical Imaging, 2013, pp. 86700H-86700H.

[5] J. H. Tan, U. R. Acharya, C. Tan, K. T. Abraham, and C. M. Lim, "Computer-assisted diagnosis of tuberculosis: a first order statistical approach to chest radiograph," Journal of medical systems, vol. 36, pp. 2751-2759, 2012.

[6] S. Jaeger, A. Karargyris, S. Antani, and G. Thoma, "Detecting tuberculosis in radiographs using combined lung masks," in Engineering in Medicine and Biology Society (EMBC), 2012 Annual International Conference of the IEEE, 2012, pp. 4978-4981.

[7] J. Jhanshy and S. Pushparani, "Automated Severity Analysis of Tuberculosis using Particle Swarm Optimization," Fuzzy Systems, vol. 7, pp. 99-102, 2015.

[8] P. A. Kamble, V. V. Anagire and S. N. Chamtagoudar, "Detection of Tuberculosis in CXR image by using MATLAB," International Research Journal of Engineering and Technology (IRJET), vol. 3(6), ISSN: 2395-0072, 2016.

[9] T. Xu, I. Cheng, and M. Mandal, "Automated cavity detection of infectious pulmonary tuberculosis in chest radiographs," in Engineering in Medicine and Biology Society, EMBC, 2011 Annual International Conference of the IEEE, 2011, pp. 5178-5181.

[10] P. Maduskar, M. Muyoyeta, H. Ayles, L. Hogeweg, L. Peters-Bax, and B. van Ginneken, "Detection of tuberculosis using digital chest radiography: automated reading vs. interpretation by clinical officers," The International Journal of Tuberculosis and Lung Disease, vol. 17, pp. 1613-1620, 2013.

[11] R. Shen, I. Cheng, and A. Basu, "A hybrid knowledge-guided detection technique for screening of infectious pulmonary tuberculosis from chest radiographs," IEEE transactions on biomedical engineering, vol. 57, pp. 2646-2656, 2010.

[12] S. Candemir, S. Jaeger, K. Palaniappan, J. P. Musco, R. K. Singh, Z. Xue, et al., "Lung segmentation in chest radiographs using anatomical atlases with nonrigid registration," IEEE transactions on medical imaging, vol. 33, pp. 577-590, 2014.

[13] H. Rachna and M. M. Swamy, "Detection of Tuberculosis bacilli using image processing techniques," International Journal of Soft Computing and Engineering (IJSCE), vol. 3, 2013.

[14] B. Castaneda, N. Aguilar, J. Ticona, D. Kanashiro, R. Lavarello, and L. Huaroto, "Automated Tuberculosis screening using image processing tools," in Health Care Exchange (PAHCE), 2010 Pan American, 2010, pp. 111-111.

[15] Y. Zhai, Y. Liu, D. Zhou, and S. Liu, "Automatic identification of mycobacterium tuberculosis from ZN-stained sputum smear: Algorithm and system design," in Robotics and Biomimetics (ROBIO), 2010 IEEE International Conference on, 2010, pp. 41-46.

[16] R. Raof, Z. Salleh, S. Sahidan, M. Mashor, S. M. Noor, F. M. Idris, et al., "Color thresholding method for image segmentation algorithm of Ziehl-Neelsen sputum slide

images," in Electrical Engineering, Computing Science and Automatic Control, 2008. CCE 2008. 5th International Conference on, 2008, pp. 212-217.

[17] M. K. Osman, M. Y. Mashor, and H. Jaafar, "Detection of mycobacterium tuberculosis in Ziehl-Neelsen stained tissue images using Zernike moments and hybrid multilayered perceptron network," in Systems Man and Cybernetics (SMC), 2010 IEEE International Conference on, 2010, pp. 4049-4055.

[18] M. Sotaquira, L. Rueda, and R. Narvaez, "Detection and quantification of bacilli and clusters present in sputum smear samples: a novel algorithm for pulmonary tuberculosis diagnosis," in Digital Image Processing, 2009 International Conference on, 2009, pp. 117-121.

[19] V. Makkapati, R. Agrawal, and R. Acharya, "Segmentation and classification of tuberculosis bacilli from ZN-stained sputum smear images," in Automation Science and Engineering, 2009. CASE 2009. IEEE International Conference on, 2009, pp. 217-220.

[20] M. G. Costa, C. F. Costa Filho, J. F. Sena, J. Salem, and M. O. de Lima, "Automatic identification of mycobacterium tuberculosis with conventional light microscopy," in Engineering in Medicine and Biology Society, 2008. EMBS 2008. 30th Annual International Conference of the IEEE, 2008, pp. 382-385.

[21] R. Khutlang, S. Krishnan, R. Dendere, A. Whitelaw, K. Veropoulos, G. Learmonth, et al., "Classification of Mycobacterium tuberculosis in images of ZN-stained sputum smears," IEEE Transactions on Information Technology in Biomedicine, vol. 14, pp. 949-957, 2010.

[22] P. Sadaphal, J. Rao, G. Comstock, and M. Beg, "Image processing techniques for identifying Mycobacterium tuberculosis in Ziehl-Neelsen stains," The International Journal of Tuberculosis and Lung Disease, vol. 12, pp. 579-582, 2008.

[23] Kusworo A, Rahmad G, Aris S, K. Sofjan F, Adi P and Ari B, "Tuberculosis (TB) identification in the Ziehl-Neelsen sputum sample in NTSC channel and support vector machine (SVM) classification," IJIRSET, vol. 2, pp. 5030-5035, 2013.

[24] I. Siena, K. Adi, R. Gernowo, and N. Mirnasari, "Development of algorithm tuberculosis bacteria identification using color segmentation and neural networks," IJVIPNS-IJENS, Vol.12, pp.9-13, 2012.

[25] https://www.youtube.com/watch?v=H0olYl2mJO0(13th december,2017).

[26] https://my.clevelandclinic.org/health/diseases/17373-pleural-effusion-causes-signs--treatment(13th december,2017).

[27] http://www.healthcommunities.com/tuberculosis/types.shtml(13th december,2017).

[28] https://www.slideshare.net/nautsilairatana/tb-diagnostics-vam-2014(15th december, 2017).

[29] F. Sana and S.A.I.Shah, " A review of Automated Screening for Tuberculosis of Chest Xray and Microscopy Images," International Journal of Scientific & Engineering Research, Vol 8(10), pp.2229-5518, 2017.

[30] K. Le, "A design of a computer-aided diagnostic tool for chest x-ray analysis," International Journal of Computer Science & Information Technology, vol. 3, pp. 212-222, 2011.

[31] C. F. F. Costa Filho, P. C. Levy, C. D. M. Xavier, L. B. M. Fujimoto, and M. G. F. Costa, "Automatic identification of tuberculosis mycobacterium," Research on Biomedical Engineering, vol. 31, pp. 33-43, 2015.

[32] H. Das and A. Nath, "An Efficient Detection of Tuberculosis from Chest X-rays," International Journal, vol. 3, 2015.

[33] A. Divekar, C. Pangilinan, G. Coetzee, T. Sondh, F. Y. Lure, and S. Kennedy, "Automated detection of tuberculosis on sputum smeared slides using stepwise classification," in SPIE Medical Imaging, 2012, pp. 83153E-83153E-9.

[34] J. Chang, P. Arbeláez, N. Switz, C. Reber, A. Tapley, J. Davis, et al., "Automated tuberculosis diagnosis using fluorescence images from a mobile microscope," Medical Image Computing and Computer-Assisted Intervention–MICCAI 2012, pp. 345-352, 2012.

[35] V. Chandrika, C. Parvathi, and P. Bhaskar, "Multi-level image enhancement for pulmonary tuberculosis analysis," International Journal of Science and Applied Information Technology, vol. 1, pp. 102-106.

[36] A. Adgaonkar, A. Atreya, A. D. Mulgund, and J. R. Nath, "Identification of Tuberculosis bacilli using Image Processing."

[37] J. M. Leibstein and A. L. Nel, "Detecting tuberculosis in chest radiographs using image processing techniques," University of Johannesburg, 2006.

[38] A. Goyal, M. Roy, P. Gupta, M. K. Dutta, and S. Singh, "Automatic detection of mycobacterium tuberculosis in stained sputum and urine smear images," Archives of Clinical Microbiology, vol. 6, 2015.

[39] M. Forero-Vargas, F. Sroubek, J. Alvarez-Borrego, N. Malpica, G. Cristóbal, A. Santos, et al., "Segmentation, autofocusing and signature extraction of tuberculosis sputum images," Photonic Devices and Algorithms for Computing IV. Proceedings, pp. 341-352, 2002.

[40] R. Khutlang, S. Krishnan, A. Whitelaw, and T. S. Douglas, "Automated detection of tuberculosis in Ziehl-Neelsen-stained sputum smears using two one-class classifiers," Journal of microscopy, vol. 237, pp. 96-102, 2010.

[41] S. Jaeger, A. Karargyris, S. Candemir, L. Folio, J. Siegelman, F. Callaghan, et al., "Automatic tuberculosis screening using chest radiographs," IEEE transactions on medical imaging, vol. 33, pp. 233-245, 2014.

[42] L. Hogeweg, C. I. Sánchez, P. Maduskar, R. Philipsen, A. Story, R. Dawson, et al., "Automatic detection of tuberculosis in chest radiographs using a combination of textural,

focal, and shape abnormality analysis," IEEE transactions on medical imaging, vol. 34, pp. 2429-2442, 2015.

[43] W. S. H. M. W. Ahmad, M. F. A. Fauzi, and W. M. D. W. Zaki, "Abnormality detection for infection and fluid cases in chest radiograph," in Electronics Symposium (IES), 2015 International, 2015, pp. 62-67.

[44] P. Maduskar, R. H. Philipsen, J. Melendez, E. Scholten, D. Chanda, H. Ayles, et al., "Automatic detection of pleural effusion in chest radiographs," Medical image analysis, vol. 28, pp. 22-32, 2016.

[45] J. Santony and J. Naam, "Infiltrate Object Extraction in X-ray Image by using Math-Morphology Method and Feature Region Analysis," International Journal on Advanced Science, Engineering and Information Technology, vol. 6, pp. 239-244, 2016.

[46] P. A. Kamble1, V. V. Anagire and S. N. Chamtagoudar, "CXR Tuberculosis Detection Using MATLAB Image Processing," International Research Journal of Engineering and Technology, Vol. 3, 2016.

[47] D.Jeevitha and J.Rajasekaran, "Histogram based tuberculosis analysis with parallel pixel processing," Journal of Recent Research in Engineering and Technology, Vol. 2, pp. 2349 –2260, 2015.

[48] R.K. Manisha and K.S. Palanisamy, "Computer-aided diagnosis of tuberculosis using chest radiographs," Discovery, Vol. 52, pp. 1012-1019, 2016.